Extending the range and reach of physically-based Greenland ice sheet sea-level projections

Heiko Goelzer[1], Constantijn J. Berends[2], Fredrik Boberg[3], Gael Durand[4], Tamsin Edwards[5], Xavier Fettweis[6], Fabien Gillet-Chaulet[4], Quentin Glaude[6,7], Philippe Huybrechts[8], Sébastien Le clec'h[8], Ruth Mottram[3], Brice Noel[6], Martin Olesen[3], Charlotte Rahlves[1,9], Jeremy Rohmer[10], Michiel van den Broeke[2], Roderik S.W. van de Wal[2,11]

[1] NORCE Research, Bjerknes Centre for Climate Research, Bergen, Norway
[2] Institute for Marine and Atmospheric research Utrecht, Utrecht University, Utrecht, the Netherlands
[3] Danish Meteorological Institute (DMI), Copenhagen, Denmark
[4] Univ. Grenoble Alpes, CNRS, IRD, Grenoble INP, IGE, 38000 Grenoble, France
[5] Department of Geography, King's College London, London, UK
[6] Laboratory of Climatology, Department of Geography, SPHERES research unit, University of Liège, Liège, Belgium
[7] Applied Computer Electronics Laboratory, University of Liège, Liège, Belgium
[8] Vrije Universiteit Brussel, Earth System Sciences and Departement Geografie, Pleinlaan 2, Brussel, Belgium
[9] Department of Earth Science, University of Bergen, Bjerknes Centre for Climate Research, Bergen, Norway
[10] BRGM, 3 av. C. Guillemin, 45060 Orléans, France
[11] Faculty of Geosciences, Department of Physical Geography, Utrecht University, Utrecht, the Netherlands

Correspondence to: Heiko Goelzer (heig@norceresearch.no)

Abstract. We present an ensemble of ice sheet model projections for the Greenland ice sheet (GrIS) that was produced as part of the European project PROTECT. The work makes use of ice sheet model (ISM) projections forced by high-resolution regional climate model (RCM) output and other climate model forcing, including a parameterisation for the retreat of marine-terminating outlet glaciers. The focus is on providing extended physically-based projections that improve our understanding of the range of GrIS future sea-level contributions and the inherent uncertainties over decadal to multi-centennial timescales. The experimental design builds on the Ice Sheet Model Intercomparison Project for CMIP6 (ISMIP6) protocol and extends it to more fully account for some of the uncertainties in sea-level projections. We include a wider range of CMIP6 climate model output, more climate change scenarios, several climate downscaling approaches, a wider range of sensitivity to ocean forcing and we extend projections beyond the year 2100 up to year 2300, including idealised overshoot scenarios. GrIS sea-level rise contributions range from 16-76 mm (SSP1-2.6/RCP2.6), 22-163 mm (SSP2-4.5) and 27-354 mm (SSP5-8.5/RCP8.5) in the year 2100 (relative to 2014). The projections are strongly dependent on the climate scenario, moderately sensitive to the choice of RCM, and relatively insensitive to the ice sheet model choice. In year 2300, contributions reach 49 to 3127 mm, indicative of large uncertainties and a potentially very large long-term response. Idealised overshoot experiments to 2300 produce sea-level contributions in a range from 49 to 201 mm, with the ice sheet seemingly stabilised in a third of the experiments. Repeating end of the 21st century forcing until 2300 results in contributions of 58-163 mm (repeated SSP1-2.6), 98-218 mm (repeated SSP2-4.5) and 282-1230 mm (repeated SSP5-8.5). The largest contributions of more than 3000 mm by year 2300 are found for extreme scenarios of extended SSP5-8.5 with unabated warming throughout the 22nd and 23rd century. We also

extend the ISMIP6 forcing approach backwards over the historical period and successfully produce consistent simulations in both past and future for three of the four ISMs. The ensemble design of ISM experiments is geared towards the subsequent use of emulators to facilitate statistical interpretation of the results and produce probabilistic projections of the GrIS contribution to future sea-level rise.

1   Introduction

The Greenland ice sheet (GrIS) has transitioned from a near zero overall mass balance before the early 1990s to rapidly increasing mass loss that is ongoing today (van den Broeke et al., 2017). The driving mechanism of this change can be largely attributed to atmospheric and oceanic warming surrounding the ice sheet, which is amplified in the Arctic region compared to the global mean (Rantanen et al. 2022). This makes the ice sheet the currently largest single cryospheric contributor to global mean sea-level rise (e.g. Fox-Kemper et al. 2021). Projecting the future evolution of the GrIS is therefore an important element in providing sea-level practitioners with relevant information for adaptation planning and providing policy makers with guidance concerning the urgent need for mitigation, in line with the PROTECT project goals (Durand et al. 2022).

Projections of ice sheet contributions to future sea-level rise have recently been organised into a global community effort under the guidance of the Ice Sheet Model Intercomparison Project for CMIP6 (ISMIP6, https://climate-cryosphere.org/about-ismip6/). The initiative provided projections for both the Greenland and Antarctic ice sheets that served as the main source of the ice sheet sea-level projections (Fox-Kemper et al. 2021) in the latest report of the IPCC, AR6. The ISMIP6 GrIS projections (Goelzer et al., 2020a) used an experimental protocol (Nowicki et al., 2016, 2020) that included a regional climate model (RCM) to dynamically downscale global climate scenarios to the ice sheet scale. While only one RCM was used for the projections in ISMIP6 for feasibility reasons, recent work has revealed that different RCMs can show widely different behaviour under future climate change (Glaude et al., 2024). This strongly suggests that fully characterising uncertainties in ice sheet projections requires a broader sampling of climate forcing uncertainty, in particular pertaining to the downscaling process. In addition, the first wave of ISMIP6 projections was forced by output from CMIP5 models (Goelzer et al., 2020a) and a subsequent update used a small subset of the then available CMIP6 models forcing (Payne et al. 2021), both under only two scenarios (RCP8.5/SSP5-8.5 and RCP2.6/SSP1-2.6). Extending the forcing to a broader range of downscaled CMIP6 climate forcing and scenarios was therefore another major concern.

The ISMIP6 projections started with year 2015 and the protocol did not provide any guidance on how ice sheet modellers should initialise to that starting point. This led to a wide range of ice sheet histories preceding the GrIS projections, with numerous models not matching observed mass changes (Goelzer et al., 2020a; The IMBIE Team, 2020; Aschwanden et al., 2021). This also created challenges in presenting and combining projected ice sheet changes with observed changes in the AR6. Since then, it has become a priority to consider the historical experiment as part of the simulation and it has been shown that extending the ISMIP6 forcing protocol over the historical period can produce GrIS projections consistent with observed mass changes (Rahlves et al., 2025a).

68   While physically-based ice sheet model simulations like those produced by ISMIP6 now form an important basis of sea-level

69   change projections, it requires statistical tools to generalise the results and make meaningful inferences. This need arises largely

70   from the limited sampling of climate model forcing, model physics and parameter choices that remain relatively sparse due to

71   practical limitations, computational cost and feasibility. A consequence is that some projections nowadays heavily rely on

72   emulators (e.g. Edwards et al., 2021; Rohmer et al. 2022; Rohmer et al. 2025; Edwards et al., 2026) to help their interpretation.

73   Designing ice sheet experiments that can serve both direct interpretation of the result and feeding into emulators has become

74   an important consideration.

75

76   This paper presents a new set of physically-based GrIS sea-level projections designed to extend the ISMIP6 effort in several

77   aspects and to inform a next generation of emulator-based projections. We describe the experimental protocol, forcing and

78   models (Sect. 2), present results (Sect. 3) and close with a discussion (Sect. 4) and conclusions (Sect. 5).

79   **2   Experimental setup**

80   **2.1   Experimental protocol**

81   The ice sheet model experiments largely follow the ISMIP6 protocol for GrIS projections, which is documented in detail

82   elsewhere (Nowicki et al., 2016, 2020; Goelzer et al., 2018, 2020a). Here, we provide a brief summary of the main principles

83   and differences. Output from selected CMIP Earth system models (ESMs) serves as boundary conditions for i) RCMs

84   (producing the surface mass and energy balance and near-surface climate fields) and ii) for a retreat parameterization for

85   marine-terminating outlet glaciers (Slater et al., 2019; 2020). These, in turn, provide forcing for ice sheet models (Figure 1).

86

87

88
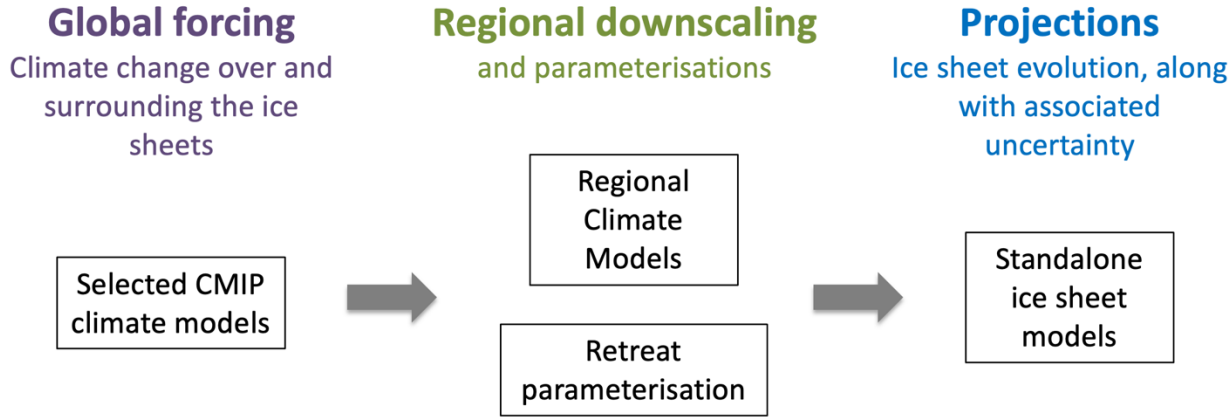
89   **Figure 1.** General forcing approach for Greenland ice sheet model projections

2.1.1 Forcing approach

The forcing from three RCMs, namely MAR (Delhasse et al., 2020), HIRHAM (Mottram et al., 2017) and RACMO (Noël et al., 2018) and from a statistical downscaling approach (Noël et al., 2022), is provided in the form of annual surface mass balance (SMB) and surface temperature (ST) anomalies relative to the period 1960-1989 (red box in Figure 2). In addition, we provide estimates of local annual vertical SMB and ST gradients, that are used to propagate dynamic ice sheet elevation changes when updating SMB and ST. The SMB forcing applied in the ice sheet model at a given time t is:

$$SMB(x,y,t) = SMBref(x,y) + aSMB(x,y,t) + dSMBdz(x,y,t) * dz(t),$$

Where SMBref [mm/yr] is the surface mass balance used by each individual ice sheet model during initialisation, aSMB [mm/yr] is the SMB anomaly, dSMBdz [mm/yr/m] is the vertical gradient of SMB and dz [m] is the elevation change since the start of the experiment. A similar approach applies to ST that can be used as boundary condition for the evolution of ice temperature in the model. Differences in SMB and ST stem from the various ESMs and scenarios used to force the three RCMs.

The retreat of marine-terminating outlet glaciers is parameterised as an empirically derived function of ocean thermal forcing (from the ESMs) and runoff (from the RCMs), both identified as the main drivers for melting of marine-based calving fronts (green box in Figure 2, Slater et al., 2019; 2020). This is a relatively crude approximation for the complex interaction between glaciers and the ocean that is poorly understood and difficult to resolve in large-scale ice sheet models. The uncertainty in this forcing is captured by a retreat parameter *kappa*, that can be expressed probabilistically and is sampled at its median (med), 25th (high) and 75th (low) percentile value (like in ISMIP6) and in extension at its 5th and 95th percentile value (cf. Figure 5a in Slater et al., 2019). In some cases, we have added control experiments without any prescribed retreat that are labelled 'pno'.

CMIP6 models
- selected based on availability
- quality check over historical period

CMIP5 models
- performance over historical period
- to maximise spread in projections

Surface mass balance forcing
- RCMs forced by CMIP models
- SMB anomalies relative to 1960-1989
- SMB elevation feedback parameterized based on d(Runoff)/dz

Outlet glacier forcing
- Prescribed outlet glacier retreat
- Empirically derived based on historical glacier retreat, ocean temperature and runoff
- κ parameter for sensitivity

Ice sheet models
- From PROTECT project partners

Figure 2. Surface mass balance and retreat forcing

112 **2.2 Regional climate model forcing**

113 The emphasis of this project is to extend the range of available forcings to a larger number of CMIP6 ESMs, scenarios (SSP1-

114 2.6, SSP2-4.5, SSP5-8.5) and to provide surface mass balance forcing from several RCMs: MAR (Delhasse et al., 2020),

115 RACMO (Noël et al., 2018) and HIRHAM (Mottram et al., 2017). In addition, we use forcing produced by a statistical

116 downscaling approach (SDBN1, Noël et al., 2016, 2020, 2022), which has been used here to translate ESM forcing from

117 CESM2-WACCM directly to the ice sheet scale. In the following, we will consider this approach included when using the

118 term RCMs. An overview of available forcing data is given in Table 1. Corresponding retreat mask forcing can be constructed

119 given sufficient output data from the RCMs and additional ESM ocean data, typically retrieved from the CMIP archives

120 (https://esgf-node.llnl.gov/projects/cmip6/). Forcing with MAR version 3.9 was produced for ISMIP6 and remained available

121 for ice sheet simulations under PROTECT.

122

123 **Table 1.** SMB forcing data available for ice sheet modellers. MARv3.9 output was produced for ISMIP6.

CMIP	ESM	SSP1-2.6 RCP2.6	SSP2-4.5	SSP5-8.5 RCP8.5
CMIP6	CESM2	MARv3.12 RACMO2.3p2	MARv3.12 RACMO2.3p2	MARv3.12
	CESM2-Leo[†]			MARv3.9 MARv3.12 RACMO2.3p2 HIRHAM5
	CESM2-WACCM	SDBN1[‡]		SDBN1[3]
	CNRM-CM6-1			MARv3.9 MARv3.12
	CNRM-ESM2-1			MARv3.9 MARv3.12
	EC-Earth3	HIRHAM5		HIRHAM5
	IPSL-CM6A-LR			MARv3.12
	MPI-ESM1	MARv3.12	MARv3.12	MARv3.12
	NorESM2-MM		MARv3.12	MARv3.12
	UKESM1-0-LL		MARv3.12	MARv3.12
	UKESM1-0-LL-Robin[†]			MARv3.12
CMIP5	ACCESS1.3			MARv3.9 MARv3.12
	CSIRO-Mk3.6.0			MARv3.9
	HadGEM2-ES			MARv3.9
	IPSL-CM5-MR			MARv3.9

	MIROC5	MARv3.9		MARv3.9
	NorESM1-M			MARv3.9

124 † pre-CMIP6 ensemble member. ‡Direct statistical downscaling of CESM2-WACCM (Noël et al., 2022).

125 **2.2.1   Required RCM data**

126 The data required to produce ice sheet model forcing were developed during ISMIP6 in collaboration with the developers of
127 MAR, the only RCM used to generate projections for the project at the time. This includes extension of the RCM forcing
128 beyond the observed ice sheet mask and producing output needed for vertical adjustment of the forcing to a changing ice sheet
129 topography. In MAR this is done with the same statistical downscaling method used to produce results at 1 km resolution
130 (Franco et al., 2012) as done in the GrSMBMIP intercomparison (Fettweis et al., 2020). In RACMO and SDBN1, vertical
131 gradients were estimated following Noël et al. (2016) combining statistically downscaled SMB components with surface
132 elevation and ice mask from the Greenland Ice Mapping Project (GIMP) DEM (Howat et al., 2014), down-sampled to 1 km
133 spatial resolution. Vertical gradients were first computed on ice-covered grid cells using SMB components and surface
134 elevation of the current grid-cell and at least five (up to eight) neighbours and further extrapolated outside the ice sheet to
135 cover the tundra region.

136 In HIRHAM5, gradients are produced at a 5 km horizontal resolution using an updated subsurface scheme (Langen et al.,
137 2017). These gradients are subsequently bilinearly interpolated to the 1 km MAR grid. Outside the observed ice mask,
138 extrapolation to cover the tundra is performed via distance-weighted averaging, followed by smoothing using weighted
139 averages of the grid points, including the eight surrounding points.

140

141 To facilitate use of RCMs and other downscaled climate forcing in PROTECT and other projects, we outline a detailed data
142 request in Appendix A.

143 **2.3   Forcing dataset preparation**

144 Output from RCMs and ESMs is collected and processed using methods established during ISMIP6. The aim is to provide a
145 consistent forcing dataset for ice sheet modellers in familiar format. It requires interpolation of RCM output to a common grid
146 at 1 km resolution, calculating anomalies and adjusting units and file formats. Retreat mask forcing is produced based on the
147 initial ice sheet mask for each individual participating ice sheet model and version. All data are provided in NetCDF format
148 following the ISMIP6 guidelines (https://theghub.org/groups/ismip6/wiki/ISMIP6-Projections-Greenland).

149 **2.4   Participating ice sheet models**

150 The ensemble includes four numerical ice sheet models that are routinely run by the participating partners for GrIS simulations
151 (IMAU, VUB, IGE, NORCE). A brief overview of the model characteristics is given in Table 2 and short model descriptions
152 are given below.

153

Table 2. Ice sheet model names and characteristics. SIA - Shallow ice approximation to the force balance, SSA - Shallow shelf approximation, HO – higher order approximation (Fürst et al. 2013), DIVA - variationally derived, depth-integrated approximation (Goldberg 2011).

Group-Model	Type	Resolutions (km)	Variants
IMAU-IMAUICE	SIA-SSA, regular grid	10, 16, 20, 30, 40	Sliding law, spinup
VUB-GISM	Regular grid	5	HO, SIA
IGE-ELMER	SSA, finite element	1 – 6 (variable)	Sliding law
NORCE-CISM	DIVA, regular grid	2, 4, 8, 16	Initial and historical SMB

157

2.4.1 IMAU-IMAUICE

The model (Berends et al., 2022) is initialised using a hybrid approach, combining a basal inversion method (Berends et al., 2023) with a paleoclimate spin-up. During the inversion phase of the initialisation, spatial patterns in basal slipperiness are iteratively adjusted until the modelled ice sheet reaches a stable state that closely matches the observed present-day ice sheet geometry (Morlighem et al., 2017) and surface velocity (doi: 10.24381/cds.0b96b838). The prescribed climate is fixed at present-day conditions: monthly mean values of 2-m air temperature and total precipitation, which are obtained from the 1950-1980 mean of the ERA5 reanalysis (Hersbach et al., 2020). The SMB is calculated from these quantities using the IMAU-ITM model, which is calibrated to RACMO2.3p2 over the 1979-2014 period (Fettweis et al., 2020). The steady-state geometry and basal slipperiness resulting from the inversion phase are then used to initialise the model during the last interglacial, 120,000 years ago. The climate evolution of the last glacial cycle is then prescribed using a matrix method (Berends et al., 2018), based on different pre-calculated GCM output for the different IMAU-ICE versions: either HadCM3 (Singarayer and Valdes, 2010), CCSM (Brady et al., 2013), or the PMIP3 best-performing ensemble mean (Scherrenberg et al., 2023). Climate evolution during the historical period is approximated by forcing the climate matrix with the Law Dome ice-core CO_2 record (MacFarling Meure et al., 2006), subjected to a 60-year smoothing representing the delayed response of the climate to changes in CO_2.

2.4.2 VUB-GISM

VUB-GISM (Huybrechts, 2002; Fürst et al., 2013; 2015) is configured either with the higher order or a shallow ice approximation to the force balance. GISM was initialised to the present-day geometry by assimilation of the observed ice thickness (Le clec'h et al., 2019). A steady state was assumed for the starting date of December 1989 using the 1960–1989 mean SMB from MAR forced by the ERA5 meteorological reanalysis climate. The iterative initialization method optimised both the basal sliding coefficient in unfrozen areas and the rate factor in Glen's flow law for frozen areas. The ice temperature and the initial velocity field needed in the initialization procedure were derived from a glacial spin-up with a freely evolving geometry over the last two glacial cycles with a synthesised temperature record based on ice-core data from Dome C, NGRIP,

GRIP and GISP2 (Fürst et al., 2015). For this spin-up experiment, a PDD model was used with an observed precipitation field derived from the Bales et al. (2009) surface accumulation for the period 1950–2000 and scaled by 5% per degree. The ice temperature and velocity fields from the "free geometry present-day" were rescaled to the observed ice thickness (Morlighem et al., 2017) and excluded peripheral ice (Citterio et al., 2013). The historical experiment is run from January 1990 to December 2014 using the yearly SMB from MAR forced by ERA5 meteorological reanalysis. For the projections, the standard retreat forcing from the ISMIP6 protocol is applied.

2.4.3 IGE-ELMER

The model is initialised using an inverse control method as in Gillet-Chaulet et al. (2012) to calibrate the basal friction coefficient field. For the momentum equations, we solve the shelfy-stream approximation with a sub-grid parameterization of the friction for partially grounded elements. The vertically averaged viscosity is constant in all simulations and is initialised using the temperature field coming from a palaeo-spin-up (125 kyr) of the SICOPOLIS model. The basal friction coefficient is constant in all transient simulations and is initialised with the control method so that the mismatch between observed and modelled surface velocities is minimum. As observations, we use a composite from the NASA Making Earth System Data Records for Use in Research Environments (MEaSUREs) Greenland Ice Sheet Velocity Map (V1) (Joughin et al., 2010). The ice sheet topography is initialised using the IceBridge BedMachine Greenland V3 data set (Morlighem et al., 2017). The ice sheet model is then relaxed for 20 years using a constant surface mass balance given by the 1960–1989 mean SMB from the regional climate model MAR v3.12 forced with ERA5 (Fettweis et al., 2017). The calving front positions are fixed during the relaxation. We use an anisotropic mesh with a horizontal resolution ranging for 1 to 6 km. For the projections, the standard ISMIP6 protocol is applied and we test the sensitivity to different friction laws: a linear friction law, Weertman friction law with m=1/3 and a parameterised Coulomb friction law.

2.4.4 NORCE-CISM

The Community Ice Sheet Model (CISM; Lipscomb et al., 2019) is run using a depth-integrated higher-order velocity solver based on Goldberg (2011) and a basal-sliding law based on Schoof (2005). The ice sheet is initialised with present-day thickness and bed topography (Morlighem et al., 2017) and an idealised temperature profile. CISM is then spun up for 5 000 years with surface mass balance and surface temperature from a 1960–1989 climatology provided by the MAR regional climate model (Fettweis et al., 2017) and with basal heat fluxes from Shapiro and Ritzwoller (2004). During the spin-up, the model is nudged toward present-day thickness by adjusting friction coefficients in a basal-sliding power law. There is no dependence of basal sliding on basal temperature or water pressure. All floating ice is assumed to calve immediately. For partly grounded cells at the marine margin, basal shear stress is weighted using a grounding-line parameterization. By the end of the spin-up, the ice thickness, temperature and velocity fields are very close to steady-state and closely match the provided observed geometry and also the observed horizontal velocity, which is not used during initialisation. For the historical period (1960–2014), the model is run forward with SMB and surface temperature anomalies, including lapse-rate corrections, from the MAR

212 simulation that provided the background climatology and with retreat forcing of various sensitivities. Basal friction coefficients
213 are held fixed at the values obtained during the spin-up. The different CISM model versions used here differ by the horizontal
214 grid resolution (2 - 16 km), by the RCM version used for spinup and historical run (MARv3.9 vs MARv3.12) and by the
215 sensitivity of the retreat parameterisation applied over the historical period.
216

2.5   Experiments

2.5.1   Ice sheet initialisation and historical run

219 Under ISMIP6 protocol, ice sheet modellers were free to initialise their model as they wish, with the aim to produce a present-
220 day state of the ice sheet that is close to observations. This procedure may involve a historical experiment that brings the ice
221 sheet into a state that is assigned to the end of 2014. In contrast to this freedom in setting up the model, the projections 2015-
222 2100 that then follow are very tightly constrained by the forcing. This is also the case for the retreat forcing, which takes the
223 individual 2014 ice mask as a reference and provides masks that impose the position of the (retreated) calving fronts forward
224 in time. For PROTECT we have extended this approach by providing retreat forcing before 2015 that is calculated from
225 reconstructions of past runoff and ocean thermal forcing (see Rahlves et al., 2025a). This allows for a consistent forcing of the
226 models in past and future and considers historical retreat of the outlet glaciers, which was an important source of mass loss
227 after 1990 (The IMBIE Team, 2020). We can now interpret the experiment leading up to 2015 as a real historical simulation.
228 The ISMIP6 practice of removing the results of an unforced control experiment from the projections is therefore not needed
229 here. Figure 3 illustrates the 2014 state of selected model versions in comparison with observations (BedMachine v3,
230 Morlighem et al., 2017).
231 The practice of including the historical experiment as part of the experimental design (which was not the case for ISMIP6)
232 should ultimately imply that any variation in the ISM modelling choices should be represented in this experiment. As a
233 consequence, each model variant would in principle require a separate historical experiment, so that modelling choices remain
234 consistent at the beginning of the projections (here in year 2015). At the beginning of the project, we did not apply this
235 constraint and most ice sheet model runs were conducted with a single historical experiment (like in ISMIP6) with medium
236 retreat sensitivity, which then branches into projections with different sensitivity. We later conducted some experiments with
237 consistent retreat forcing sensitivity with NORCE-CISM (cf. list of ISM experiments in Appendix B).
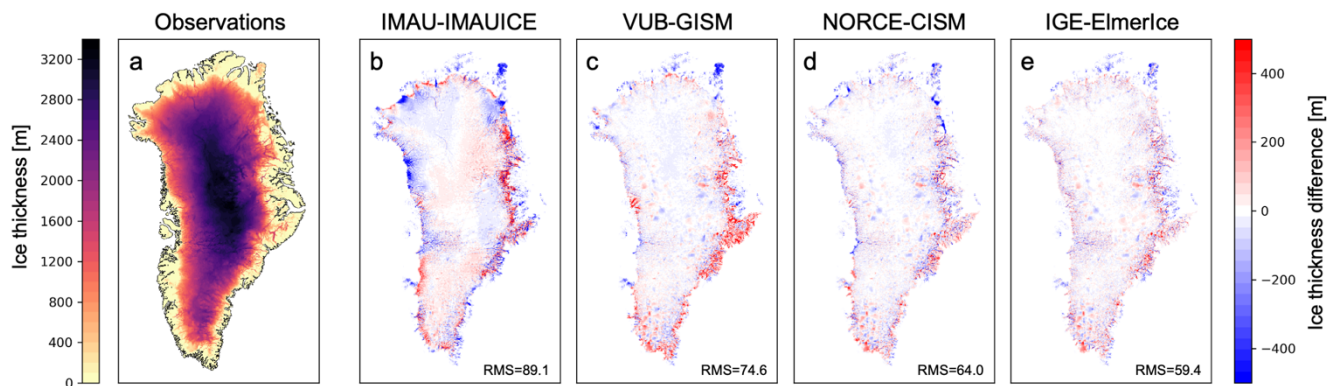
Figure 3. Ice thickness comparison. (a) Present day observations (Morlighem et al., 2017). (b-e) Difference of modelled 2014 ice thickness compared to observations for one model version per group. The root mean square (RMS) difference to the observations in m is given in the lower right of panels b-e.

2.5.2   Future projections to year 2100

The future projections from 2015 to 2100 follow the ISMIP6 forcing protocol with SMB anomalies and retreat forcing applied as described in Sec. 2.1.1. With the available forcing described in Sec. 2.3, we obtained output from 14 different global models, forced with three different scenarios (SSP1-2.6, SSP2-4.5, SSP5-8.5) and downscaled with three RCMs and one statistical downscaling method.

2.5.3   Extensions after year 2100

Few CMIP6 models have carried out the scenarioMIP extensions (O'Neill et al., 2016) to 2300, and even fewer have provided 6-hourly output typically required for RCMs to downscale the data. We have currently only three examples of ice sheet forcing with what we will refer to as 'natural extensions' beyond 2100 from the ESMs IPSL-CM6A-LR (for scenarioMIP SSP5-8.5-ext) and CESM2-WACCM (for scenarioMIP SSP5-8.5-ext and scenarioMIP SSP1-2.6-ext). While SSP1-2.6-ext stabilises to a CO_2 concentration well below 500 ppm, SSP5-8.5-ext stabilises towards a CO_2 concentration of about 2200 ppm, roughly double its value at year 2100. CESM2-WACCM has been statistically downscaled with SDBN1 (not requiring 6-hourly output) and IPSL-CM6A-LR has been dynamically downscaled with variants of MARv3.12. There is one extension to 2200 with MARv3.12 downscaling IPSL-CM6A-LR under scenario SSP5-8.5/SSP5-8.5-ext using the same approach as for the other experiments. The MAR modellers questioned the validity to continue downscaling the relatively strong climate forcing from IPSL-CM6A-LR SSP5-8.5-ext at a fixed present-day topography beyond 2200, given that the ice sheet geometry should have considerably changed by then, hence impacting SMB (Delhasse et al., 2024). We have therefore performed two additional pilot experiments with different topography updates extending to 2300 (MARv3.13-e05 and MARv3.13-e55). The construction of these forcings is described in more detail in Appendix C. The retreat mask forcing can in principle be constructed in the same way as for the experiments extending to 2100. However, the underlying assumptions of the parameterisation may not hold for the very large retreat distances produced under sustained very strong warming to 2300. Because of that we have

263   already limited the retreat sensitivity to the 25-75 percentile range for the natural extensions, but caution that these simulations
264   show higher uncertainty.

265   In addition to the natural extensions, we have designed schematic extensions of the forcing data to the year 2300 to evaluate
266   the longer-term response of the ice sheet for a broader range of ESMs. The first set of extensions is carried out by repeating
267   the forcing of the last ten available years (2091-2100) in randomised order and keeping the retreat mask of year 2100 constant.
268   For a second type of schematic extension, we have designed overshoot scenarios mimicking SSP5-3.4-OS by reusing the
269   regular SSP5-8.5 forcing before 2100 and simulating a climate cooling and corresponding increase of the SMB until 2300.
270   These overshoot scenarios are constructed using global mean temperature as a proxy for the temperature and SMB evolution
271   by sampling existing yearly forcing data until 2055 and reorganising them to new time series until 2300. The shape of the
272   global temperature proxy evolution is parameterised and has been calibrated to a few existing ESM results (CESM2-WACCM,
273   IPSL-CM6A-LR, MRI-ESM2-0) for overshoot scenario SSP5-3.4-OS. The resulting time series are illustrated in Appendix C.
274   Aside from the obvious shortcoming that the latter two are schematic extensions, the formulation of the retreat forcing implies
275   a constant mask for stabilising the forcing, which may underestimate the retreat. Furthermore, another problem on this
276   timescale in general may be that the climate response to changing ice sheet geometry is not properly accounted for. Alternative
277   prolongations could be envisioned and thus the current approaches should be considered pilot experiments and not a guide to
278   produce realistic scenarios.

279 **2.6   Data request for ice sheet model output**

280   The requested ice sheet model data consists of the most important diagnostic output at annual time resolution, such as ice
281   thickness, bedrock and surface topography, horizontal velocities and integral mass balance terms. We are following the ISMIP6
282   data request format (https://theghub.org/groups/ismip6/wiki/ISMIP6-Projections-Greenland).
283

284 **2.7   Ensemble design**

285   The collection of forcing data covers a wide range of variations across different ESMs and greenhouse gas (GHG) scenarios,
286   but ultimately represents an 'ensemble of opportunity'. This is even more true for the selection of RCMs and ISMs, which is
287   limited to available models in the consortium. PROTECT has therefore conceptualised and operated from the beginning a
288   modelling strategy that embeds the physically-based modelling into a wider framework allowing for a statistically meaningful
289   probabilistic interpretation of the results.

290   In order to facilitate the sampling strategy in that framework, experiments in the ensemble are labelled by 6 characteristics that
291   are colour-coded in Figure 4 and given in square brackets in the following. Setting up a specific ice sheet simulation requires
292   climate forcing (SMB and ST) for a given choice [Global model, GHG scenario, Regional model] and retreat mask forcing for
293   a given choice [Global model, GHG scenario, Regional model, Retreat sensitivity]. We furthermore have different ice sheet
294   models built on a certain [Code base] (here referred to by the ISM name) and they are operated using certain modelling

295 [Choices] (initialization strategy, approximations, parameterizations, parameter choices). In our current approach, different

296 sets of modelling choices are summarised and assigned to a specific model version number. However, the impact of specific

297 modelling choices could be further analysed e.g., by using the technique described by Rohmer et al. (2022; 2025).

298
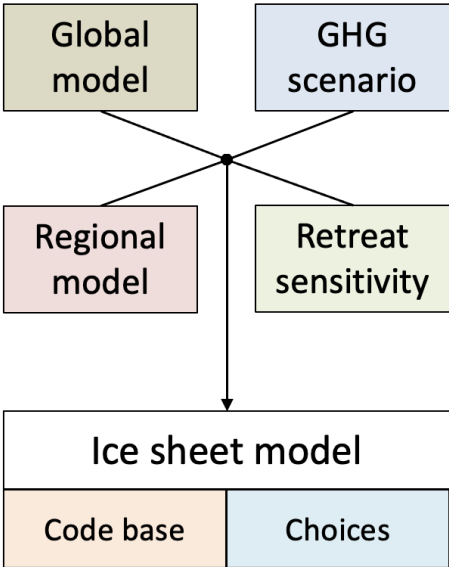
299

300 **Figure 4.** Forcing and model options relevant for the larger ensemble design.

301

302 The current set of results discussed below is a broad sampling of the available forcings and parameter choices to cover a wide

303 range of possible projections and their uncertainties. Based on feedback from the researchers running emulators using these

304 results, we have iteratively updated the ensemble with additional simulations to refine the sampling for specific choices where

305 needed. The repeated extensions and overshoot scenarios are examples of additional experiments that were deemed important

306 to improve the emulator performance for predictions up to 2300.

307 **3   Results**

308 The following results are presented as an overview of available ISM simulations and provide insight into the typical ranges

309 and main uncertainties. We have produced 1472 individual ice sheet model projections that form the ensemble of GrIS results.

310 An overview of the used ISM model versions is given in Table A2. Sea-level contributions are calculated taking into account

311 density (and bedrock adjustment for IMAUICE) following Goelzer et al. (2020b).

312 Figure 5 illustrates the typical time-dependence of the projections from the ensemble, with output from one model version per

313 group under the range of ESM and RCM forcing with median outlet glacier retreat sensitivity. It also shows historical

314 simulations of various lengths for the different ISMs. Under this forcing, which includes scenarios SSP1-2.6, SSP2-4.5 and
315 SSP5-8.5 for various ESMs, all sea-level contributions are increasing and positive by the year 2100. Judging by average mass
316 loss rates over the last 30 years, none of the simulations shows signs of ice sheet stabilisation (zero or positive mass change)
317 towards the end of the experiment, but rather continued mass loss, suggesting larger to much larger contributions for time
318 scales beyond 2100.
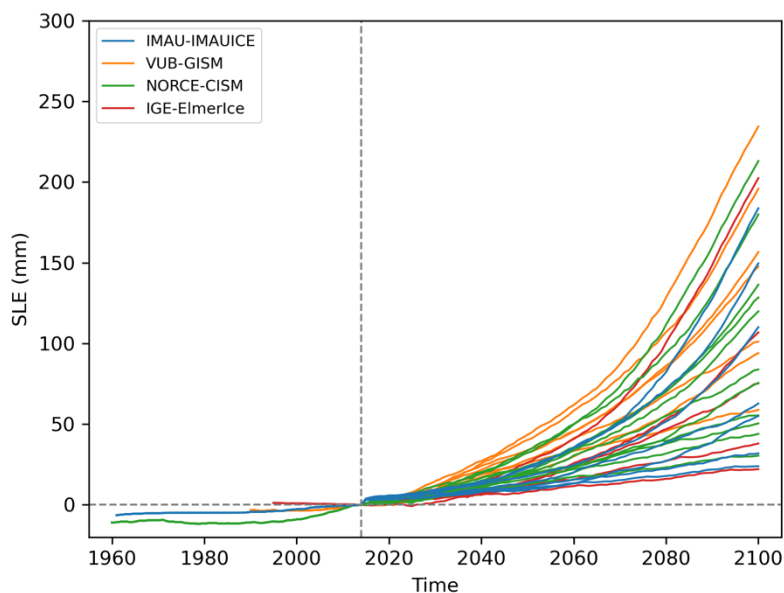
319
320 **Figure 5.** Projected sea-level contribution from the GrIS until 2100 from the four participating ice sheet models (one model version per
321 group), median retreat sensitivity and forcings produced specifically for PROTECT (MARv3.12, RACMO2.3p2, HIRHAM5). The aim of
322 this figure is to illustrate the range and distribution of the projections, not individual members.

323 Results for the year 2100 of the whole ensemble of projections with all available scenarios, ESMs, RCMs and ISMs under five
324 different retreat sensitivities (5th percentile, high, med, low, 95th percentile) are summarised in Figure 6. We have not included
325 results for the experiments that continue to 2200 and 2300 here, which are instead shown in Figure 9 with results at the
326 respective ends of the simulations. The contributions in the year 2100 (relative to 2014) lie in a range between 16 and 354 mm,
327 with the largest numbers from experiments that combine high climate sensitivity (UKESM1-0-LL variants) and very high
328 retreat sensitivity (5th percentile). The corresponding global mean temperature anomalies as diagnosed from the ESMs are
329 given in Figure S1 in the supplement.
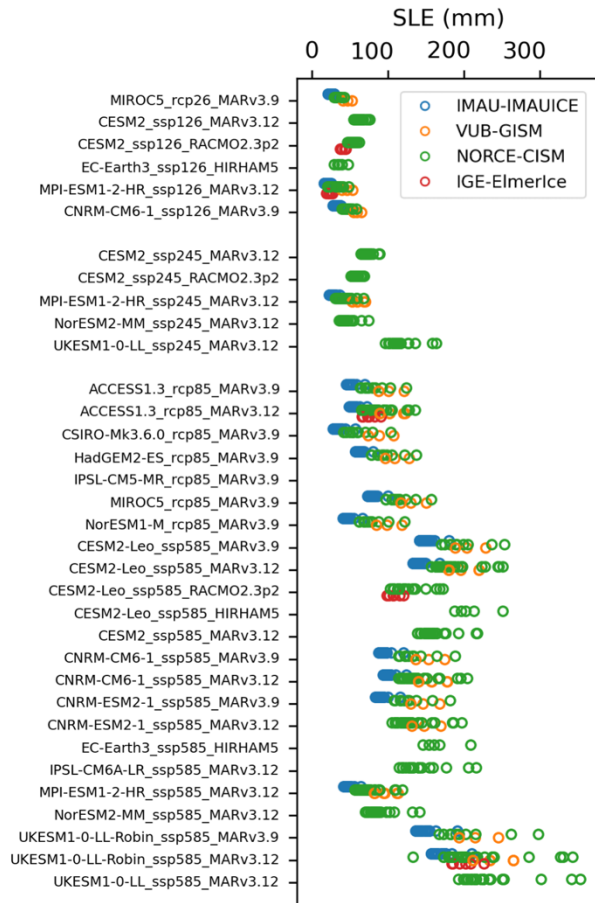
Figure 6. Overview of produced GrIS sea-level projections for the year 2100 from 4 ice sheet models (23 different model versions) and 5 retreat sensitivities (med, high, low, p95, p05).

Figure 7 illustrates ISM results of the runs to 2100 sorted by different categories. The comparison between ISMs (a), RCMs (b), scenarios (c) and CMIP iterations (d) shows primarily the sampling frequency across the ensemble. Unequal sampling limits the direct interpretation of the results, but some conclusions can be drawn, nevertheless. The range of results for the different ISMs is largely similar (Figure 7a) and only larger for CISM because a wider range of retreat parameters (5th - 95th percentile range) was sampled with this model. Simulations forced with regional models MAR and HIRHAM5 (Figure 7b) show higher contributions under high climate forcing compared to RACMO, which is in line with SMB results discussed recently (Glaude et al, 2024): the contrasted response to warming of the utilised RCMs primarily stems from differences in projected runoff, which is amplified by the positive melt-albedo feedback.

The full scenario ranges (Figure 7c) of projected sea-level contributions from the GrIS by the year 2100 (relative to year 2014) are 16-76 mm (SSP1-2.6/RCP2.6), 22-163 mm (SSP2-4.5) and 27-354 mm (SSP5-8.5/RCP8.5). For the narrower range of the

retreat parameter (25th - 75th percentile range as in ISMIP6 and performed by all ISMs), the (upper) scenario ranges are reduced to 22-127 mm (SSP2-4.5) and 27-265 mm (SSP5-8.5/RCP8.5). In summary, these results indicate a very large range of sea-level contributions in particular under forcing scenario RCP8.5/SSP5-8.5. Figure 7d shows an increased sensitivity from CMIP5 to CMIP6, confirming earlier results (e.g. Hofer et al., 2020; Payne et al., 2021), although unequal sampling is an additional factor.
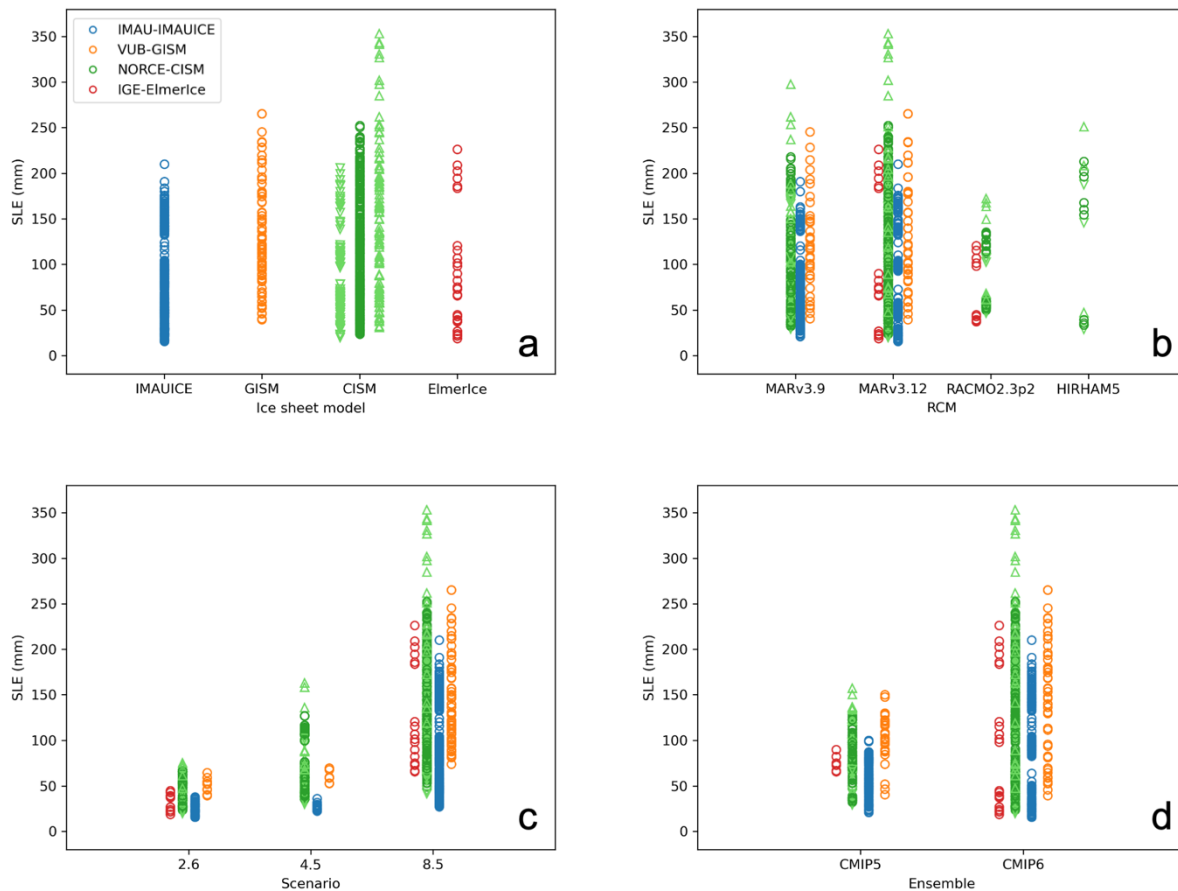
Figure 7. Sea-level contribution by year 2100 from the GrIS sorted by a) ice sheet model, b) regional climate model, c) scenario and d) CMIP ensemble. The colour legend is the same for all panels. Scenarios labelled '2.6' in c) include SSP1-2.6 and RCP2.6 and '8.5' includes SSP5-8.5 and RCP8.5.Triangular light green markers for NORCE-CISM indicate experiments with extreme values of the retreat parameter kappa in the 5th percentile (upward-pointing) and 95th percentile (downward-pointing).

Uncertainty in the projections arises from the climate forcing (different ESMs, scenarios), the translation of the forcing to the ice sheet scale (RCMs/downscaling, retreat parameterisation) and from the ISMs themselves. We have quantified these uncertainty ranges by comparing experiments with one of the factors modified at a time and averaging over available subsets.

359   Under SSP5-8.5/RCP8.5 forcing, the ESM choice explains a range of 130 mm (cf. Figure 7c), compared to a range of 84 mm

360   for RCMs (cf. Figure 7b), 50 mm for ISMs (cf. Figure 7a) and 13 mm for retreat forcing (25th - 75th percentile range).

361   Figure 8a shows results for a schematic prolongation to 2300 for one of the ice sheet models with repeated SMB forcing and

362   constant retreat mask after year 2100. It illustrates that sea-level contributions from Greenland continue to increase well beyond

363   year 2100 even under stabilised forcing. Contributions can exceed 1.2 m (under very high retreat forcing) by 2300 for

364   prolonged SSP5-8.5/RCP8.5 but may stabilise for prolonged SSP1-2.6/RCP2.6 somewhere below 200 mm. The scenario

365   ranges with repeated forcing are 58-163 mm (repeated SSP1-2.6), 98-218 mm (repeated SSP2-4.5) and 282-1230 mm (repeated

366   SSP5-8.5).

367   Results from the schematic overshoot scenarios, mimicking SSP5-3.4-OS (Figure 8b) with sea-level contributions at year 2300

368   in a range between 49 and 201 mm, show stabilisation for three out of the nine experiments (CESM2-WACCM SDBN1,

369   CESM2-Leo RACMO2.3p2, NorESM2-MM MARv3.12), while the others have an ongoing near-linear mass loss trend at the

370   end of the experiments by 2300. The natural extensions to 2300 (Figure 8c) for CESM2-WACCM SDBN1 show a range

371   between 92 mm (SSP1-2.6) and 3127 mm (SSP5-8.5), indicating a strong dependence on the climate forcing. large

372   uncertainties and a potentially very large long-term response. Results for IPSL-CM6A-LR SSP5-8.5-ext show that including

373   a topography update (MARv3.13-e55) leads to a 6% larger contribution in 2300 compared to calculating the SMB for a fixed

374   surface elevation (MARv3.13-e50). This is in addition to the parameterised SMB-height feedback active in both experiments.

375   For the natural extensions (Figure 8c) we also show the corresponding global mean temperature anomalies as diagnosed from

376   the ESMs (Figure 8d) to put the results for the extreme warming scenarios into perspective.
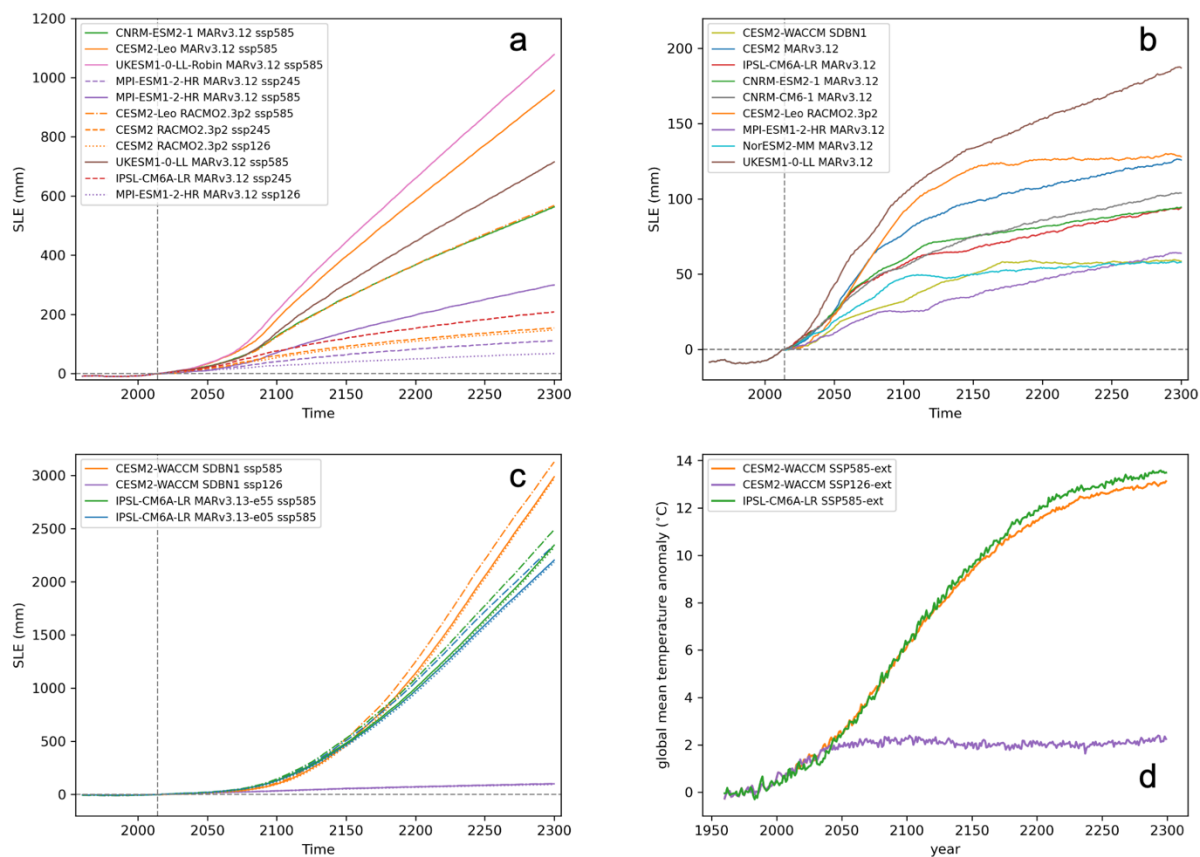
Figure 8. Extensions to 2300 with NORCE-CISM for various ESMs/RCMs with median values of retreat parameter kappa for a) repeated forcing after 2100 and b) overshoot scenario mimicking SSP5-3.4-OS. c) Natural extensions with CMIP6 forcing until 2300 with median (solid), high(dot-dashed) and low (dotted) values of retreat parameter kappa. For scenario SSP1-2.6, experiments with various values for kappa are largely overlapping and difficult to distinguish. Extensions to 2200 are overlapping with the respective continuations to 2300 and are not shown. d) ESM global mean temperature anomaly relative to 1960-1989 for the experiments in c.

Figure 9 summarizes results at the end of the experiments for all schematic prolongations to 2300 (overshoot: o2300 and repeat: r2300) and also includes the natural extensions to 2200 and 2300 for CESM2-WACCM and IPSL-CM6A-LR. Note that results for the overshoots and lower scenarios on the left in Figure 9 are displayed on a different vertical scale compared to results under the high scenario on the right.

388
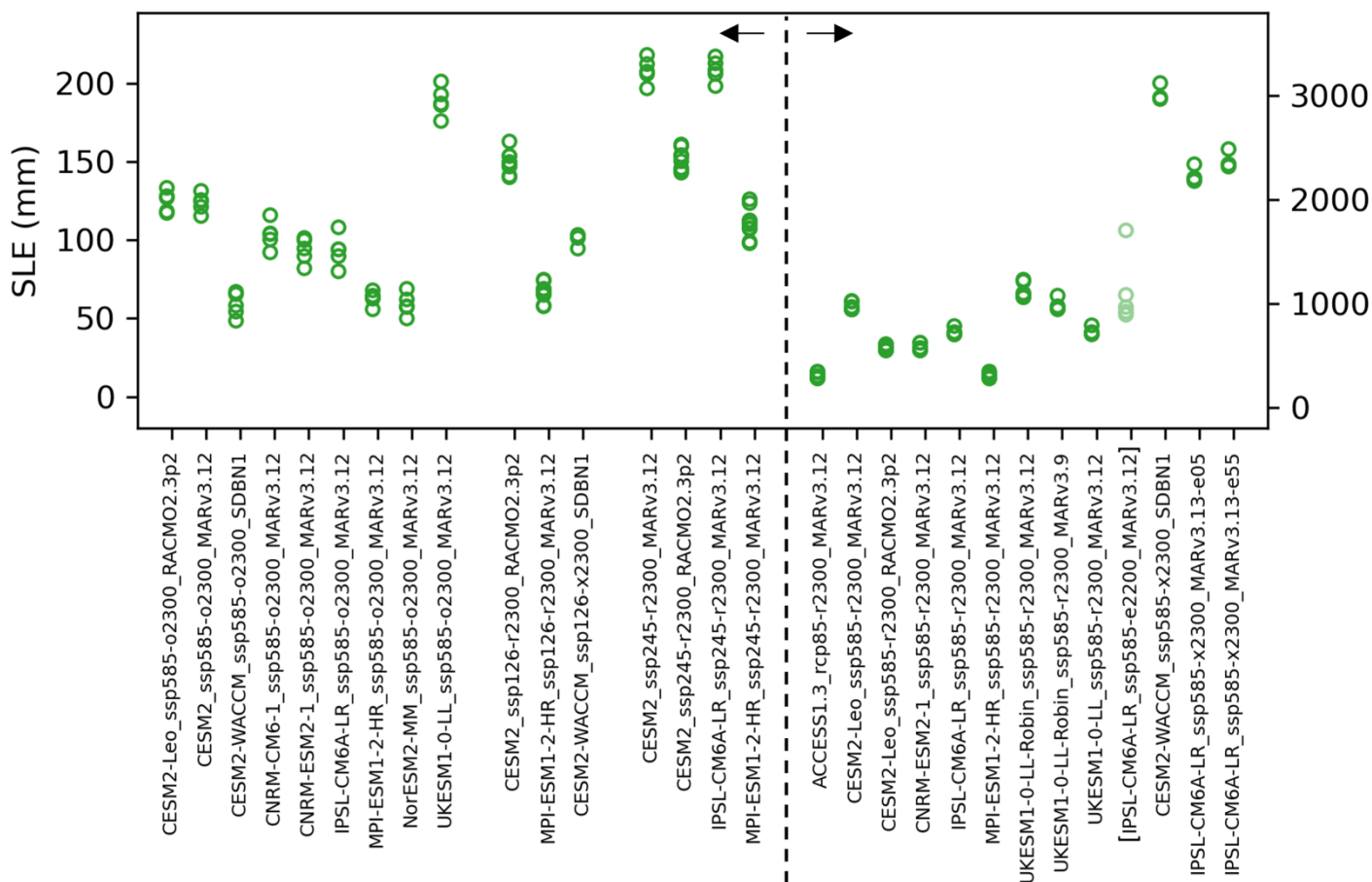
389 **Figure 9.** Results for extensions to the year 2300 with NORCE-CISM for various ESMs/RCMs. o2300 - overshoot scenario, r2300 - repeated
390 forcing, x2300 – regular ScenarioMIP extension. Experiment e2200 in brackets and with lighter colour is a regular ScenarioMIP extension
391 to 2200. The rightmost experiment forced with MARv3.13-e55 has a topography update during the MAR simulation. Note different vertical
392 scaling left (overshoot runs and scenarios SSP1-2.6 and SSP2-4.5) and right (SSP5-8.5/RCP8.5) from the dashed vertical line.

393

394 **4   Discussion**

395 For the scenarios and forcings covered in both ensembles and for the same range of the retreat parameter (25th - 75th percentile

396 range), our ranges of projected sea-level contributions at 2100 (16-67 mm for SSP1-2.6/RCP2.6, 27-265 mm for SSP5-

397 8.5/RCP8.5) largely overlap with ISMIP6 results (11-58 mm for SSP1-2.6/RCP2.6, 35-250 mm for SSP5-8.5/RCP8.5; Payne

398 et al., 2021). Slightly different ranges here are due to less ISMs, but also due to additional ESMs and RCMs. Including a wider

399 range of the retreat parameter (5th - 95th percentile range) has led to a larger upper end of the full scenario ranges presented

here as 16-76 mm (SSP1-2.6/RCP2.6), 22-163 mm (SSP2-4.5) and 27-354 mm (SSP5-8.5/RCP8.5). We have added 159 experiments for the intermediate scenario SSP2-4.5, that was not represented in ISMIP6. Inclusion of these results of an intermediate scenario does not increase the total range of projections but adds additional information for the subsequent emulation. Results for experiments with the same climate model (CESM2-Leo) but different RCMs (MAR, RACMO, HIRHAM) mirror the results from a comparison of the underlying SMB (Glaude et al., 2024), with considerable differences in the projected sea-level contribution due to the choice of RCM. In addition, a larger relative contribution from experiments forced with HIRHAM here compared to the SMB results (Glaude et al., 2024) is related to the way SMB is extended beyond the ice sheet mask and how the vertical gradients are determined for parameterising the SMB-height feedback. In combination, this highlights the urgent need to include uncertainty due to climate downscaling from global to ice sheet scale in the projections, which was likely under-represented in ISMIP6 due to the use of only one RCM and only one method to take the SMB-height feedback into account.

Uncertainties in the projections in this 'ensemble of opportunity' arise from sampling of ESMs, RCMs, ISMs and retreat parameters, which implies that statistically meaningful interpretation of the raw model output is challenging. We have therefore mostly limited the interpretation of results to typical ranges and leave finer-grained analysis to downstream efforts (e.g. Rohmer et al., 2024, 2025; Edwards et al., 2021; 2026). Under the high forcing scenario SSP5-8.5/RCP8.5, global climate model uncertainty (here choice of ESM) is dominating and explains a total range of 130 mm in the projections to 2100. This is compared to a range of 84 mm for choice of RCM (not sampled in ISMIP6), and 50 mm for the choice of ISM, which is similar to ISMIP6, despite the smaller number of ISMs in the present work. The range of 13 mm for retreat forcing (25th - 75th percentile range) is slightly smaller compared to ISMIP6 (19 mm), but increases considerably to 52 mm when extending to the 5th - 95th percentile range that we have explored here in addition.

Extending the forcing and the simulations backwards over the historical period is an important improvement compared to ISMIP6 and will eventually allow for a better comparison between observations and models. We have not attempted here to perform specific experiments that quantify the effect of including a real historical experiment on the projections, but results by Rahlves et al. (2025a) give indications that the impact on the projected sea-level contribution is minor.

Schematic extensions with repeated forcing to 2300 from a subset of ESMs (and only one ice sheet model) show an upper range of contributions exceeding 1.2 m for prolonged SSP5-8.5/RCP8.5 and potentially stabilising contributions for prolonged SSP1-2.6/RCP2.6 below 25 cm. These results are given with the caveat of the underlying schematic experimental setup and a limited ensemble size. In comparison, regular ScenarioMIP extensions under scenario SSP5-8.5-ext that we have for two global models (IPSL-CM6A-LR, CESM2-WACCM) produce contributions in the year 2300 exceeding 2.5 m and 3 m, respectively. This is in strong contrast to results under CESM2-WACCM SSP1-2.6-ext with only 92 mm, underlining that the climate scenario is the dominant source of uncertainty. We also emphasise that the natural extensions to 2300 lead to considerably higher contributions compared to the extensions with repeated forcing, indicating that these scenarios are very different and shouldn't be conflated. It also underlines an urgent need for more ESM output going to 2300. On these timescales and under such high forcing, feedbacks between ice sheet and climate and how they are taken into account become first-order effects and

434 introduce large uncertainties. In our standalone ice sheet modelling approach, the lack of proper climate feedbacks is an
435 important limitation that may be addressed with interactive coupling of ESMs and ISMs (e.g. Muntjewerf et al., 2020; Smith
436 et al., 2021; Goelzer et al., 2025). In addition, the retreat forcing approach has to be considered with caution for extended time
437 periods in particular under high forcing scenarios. Combined, these results indicate that standalone ice sheet simulations well
438 beyond year 2100 likely require modifications to the ISMIP6 forcing protocols and new methods to account for a changing ice
439 sheet geometry (e.g. Goelzer et al., 2020c; Delhasse et al., 2024; Rahlves et al., 2025b). Nevertheless, the experiments with
440 repeated forcing give an approximate idea of how stabilising forcing (and climate) at different levels could play out. On the
441 considered timescale, stabilising the forcing has the effect of stabilising the rate of change, not the ice sheet itself (unless the
442 rate is close to zero). Results from the schematic overshoot scenarios, mimicking SSP5-3.4-OS, were added specifically to
443 provide the emulator with additional, complementary information on ice sheet changes under forcing that does not follow a
444 continuous increase in temperature. Results under this forcing show that three (CESM2-WACCM SDBN1, CESM2-Leo
445 RACMO2.3p2, NorESM2-MM MARv3.12) out of the nine experiments with different climate model forcing produce what
446 seems like a stabilising GrIS towards 2300.

447 Creating this ensemble with a relatively small group of ice sheet modellers bears the risk of underestimating an important part
448 of the ISM uncertainty. We anticipate this potential gap to be closed by ISMIP7 and other follow-up initiatives. The advantage
449 of a smaller group of modelers that we have exploited in this work lies in a more flexible and adaptable experimental design.
450

5   Conclusions

452 We have produced a large ensemble of Greenland ice sheet projections with four different ice sheet models under various
453 forcings drawn from a wide range of ESMs, scenarios, RCMs, and retreat parameters. Uncertainty in the ice sheet models is
454 furthermore sampled with various model versions that differ by horizontal grid resolution, applied sliding law, and initial
455 states. Under high forcing, the largest contributor to the uncertainty is the choice of ESM, followed by the RCM and ISM.
456 RCM uncertainty, or more generally, uncertainties in the climate downscaling process need to be better quantified in the future.
457 This contribution to the European project PROTECT extends the projections of ISMIP6 in several important regards, with an
458 additional, intermediate scenario, several different RCMs, and more CMIP6 models. Results from different extensions up to
459 2300 give a perspective on challenges for standalone simulations on this time scale.

Appendix A: Data request for climate model output used as ice sheet forcing

461 This section describes the climate model output required to construct ISMIP6-type ice sheet forcing for Greenland ice sheet
462 projections.

463 **Surface mass balance (SMB):** annual cumulative SMB [mm/yr w.e.]

464 Like most variables, the SMB needs to be extended outside of the observed ice sheet mask to accommodate ice sheet models

465 with a slightly larger than observed footprint. See main text for details on how this was done in the different downscaling

466 procedures.

467 **Vertical gradients of runoff:** annual mean slope of the local runoff-elevation gradients [mm/yr w.e. per m].

468 This variable is needed to parameterise the SMB-height feedback in ice sheet models. The gradients are expected to be

469 predominantly negative as runoff generally declines with elevation and should be masked to 0 where no runoff is present. This

470 variable has to be relatively smooth. Using gradients in runoff rather than gradients in SMB to parameterize the SMB-height

471 feedback is chosen because precipitation does not have consistent gradients with elevation. Extended outside of the observed

472 ice sheet margin.

473 **Skin temperature (Tskin):** annual mean skin temperature [degree C]

474 Used to force the thermodynamic ice sheet solution at the upper boundary. Extended outside of the observed ice sheet margin.

475 **Vertical gradients of Tskin:** annual mean **slope** of the local temperature-elevation gradient [degree C per m].

476 This variable is used to apply a lapse-rate correction of the temperature boundary condition with changing surface elevation.

477 This variable should be relatively smooth. Extended outside of the observed ice sheet margin.

478 **Runoff:** monthly cumulative runoff [mm/yr w.e.].

479 This variable is used in combination with ocean thermal forcing to derive the outlet glacier retreat parameterization. As it is

480 based on the observed geometry, this is the only variable that does not need to be extended over the tundra.

481 **Ocean thermal forcing:** We need to know the exact model version of the forcing ESM so we can extract matching ocean data

482 from the CMIP archive.

483

484 Because we calculate anomalies relative to the period 1960-1989, SMB and Tskin have to cover the historical period (1960-

485 2014) in addition to the projection period (2015-2100). All other data should cover at least the projection period (2015-2100).

486 In addition, for climate forcing data to be used for ice sheet model initialisation and historical experiments, it should be

487 provided over the historical period from 1950 under ERA5 forcing or another reanalysis product.

488 **Appendix B: List of ISM projections**

489 **Table B1.** Ice sheet model versions and number of experiments. Bold model versions are shown in Figure 3 and 5.

490 Linear - linear sliding law, Weertman - Weertman sliding law (m=1/3), ZI - Zoet-Iverson sliding law, RC - regularised

491 Coulomb sliding law, PMIP3 - PMIP3 ensemble mean forcing for spinup, HadCM3 - HadCM3 forcing for spinup, CCSM -

492 CCSM forcing for spinup, MARv3.9 - initialised with MARv3.9, MARv3.12 - initialised with MARv3.12, Num - number of

493 experiments for different forcings (ESM, scenario, RCM, retreat).

Group	Model	Resolution (km)	Variant	Num
IGE	ElmerIce2	1 - 6	Linear	14

	ElmerIce3	1 - 6	Weertman	15
IMAU	IMAUICE1	40	ZI, PMIP3	57
	IMAUICE2	30	ZI, PMIP3	57
	IMAUICE3	20	ZI, PMIP3	57
	IMAUICE5	10	ZI, PMIP3	57
	IMAUICE6	20	ZI, HadCM3	57
	IMAUICE7	20	ZI, CCSM	57
	IMAUICE8	20	RC, PMIP3	57
NORCE	CISM02-MAR39	2	MARv3.9	36
	CISM04-MAR312	4	MARv3.12	48
	CISM04-MAR39	4	MARv3.9	69
	CISM04c-MAR39	4	MARv3.9, consistent[†]	95
	CISM04e-MAR312	4	MARv3.12, extension to 2200	5
	CISM04-MAR312	4	MARv3.12	4
	CISM08-MAR312	8	MARv3.12	48
	CISM08-MAR39	8	MARv3.9	115
	CISM08c-MAR39	8	MARv3.9, consistent[†]	95
	CISM16-MAR312	16	MARv3.12	48
	CISM16-MAR39	16	MARv3.9	100
	CISM16c-MAR312	16	MARv3.12, consistent[†]	110
	CISM16oc-MAR39	16	MARv3.9, overshoot to 2300	45
	CISM16t-MAR39	16	MARv3.9, repeat to 2300	65
	CISM16tc-MAR39	16	MARv3.9, repeat to 2300, consistent[†]	59
	CISM16xc-MAR12	16	MARv3.12, extension to 2300, consistent[†]	24
VUB	**GISMHOMv1**	5	Higher-order model	57
	GISMSIAv1	5	Shallow ice approximation	21

494 [†] retreat sensitivity consistent between historical and projection.

Appendix C: Construction of extensions until 2300.

Extensions under climate forcing IPSL-CM6A-LR SSP5-8.5 have been downscaled with MARv3.13, which is largely similar to v3.12. The only difference is a small correction of albedo as a function of the liquid water content of the surface snowpack. Experiment MARv3.13-e05 uses SMB forcing produced at a fixed topography, as for the other experiments. In addition, we have experiment MARv3.13-e55, which uses SMB forcing produced at a changing topography. The topography change was produced by running two iterations between MAR and CISM with consecutive update of SMB and topography. The processing steps were the following:

502  1. Run MARv3.13 forced with IPSL-CM6A-LR SSP5-8.5 to 2300, where a quarter of the cumulated SMB anomaly is

503   used to update the topography. This underestimates the topography change compared to a theoretical fully-coupled

504   experiment by around a factor 4, so it is close to no update of the topography.

505  2. Run CISM with the SMB in 1.

506  3. Run MARv3.13 forced with IPSL-CM6A-LR SSP5-8.5 to 2300 with topography changes taken every 10 years from

507   2070 forward from 2.

508  4. Run CISM with the SMB in 3.

509

510 Schematic extension of forcing between 2100 and 2300 based on existing data until 2100.

511 **Repeat scenarios**. The forcing until 2100 is the same as the corresponding scenario. From 2101 – 2300 the forcing is randomly

512 repeated by shuffling the last 10 years of existing data (2091-2100). The following indices are used.

```
513  year = 2101, 2102, 2103, […], 2298, 2299, 2300 ;
514  shuffled_time_repeat = 2093, 2099, 2095, 2100, 2092, 2097, 2098, 2094,
515     2091, 2096, 2100, 2097, 2099, 2095, 2096, 2091, 2093, 2098, 2094, 2092,
516     2099, 2095, 2094, 2096, 2091, 2097, 2100, 2093, 2092, 2098, 2100, 2095,
517     2098, 2094, 2093, 2097, 2092, 2099, 2096, 2091, 2097, 2098, 2099, 2093,
518     2095, 2100, 2092, 2096, 2091, 2094, 2098, 2091, 2094, 2100, 2099, 2092,
519     2093, 2096, 2095, 2097, 2100, 2094, 2091, 2096, 2095, 2093, 2092, 2099,
520     2097, 2098, 2100, 2098, 2091, 2096, 2093, 2092, 2099, 2094, 2097, 2095,
521     2094, 2097, 2095, 2098, 2093, 2092, 2096, 2099, 2100, 2091, 2097, 2095,
522     2092, 2094, 2100, 2098, 2099, 2091, 2096, 2093, 2093, 2091, 2096, 2095,
523     2097, 2099, 2098, 2092, 2094, 2100, 2097, 2100, 2098, 2096, 2091, 2094,
524     2099, 2092, 2093, 2095, 2091, 2099, 2100, 2093, 2095, 2094, 2092, 2098,
525     2096, 2097, 2094, 2097, 2095, 2099, 2092, 2098, 2096, 2093, 2100, 2091,
526     2094, 2098, 2093, 2097, 2092, 2100, 2096, 2095, 2091, 2099, 2095, 2091,
527     2096, 2100, 2094, 2097, 2093, 2092, 2098, 2099, 2091, 2094, 2092, 2097,
528     2096, 2100, 2098, 2093, 2099, 2095, 2096, 2091, 2094, 2093, 2098, 2097,
529     2092, 2100, 2095, 2099, 2098, 2091, 2100, 2092, 2097, 2094, 2096, 2093,
530     2099, 2095, 2095, 2096, 2091, 2100, 2099, 2093, 2094, 2092, 2097, 2098;
```

531
532
533 **Overshoot scenarios**.

534 The schematic overshoot scenario mimicking SSP5-3.4-OS are based on the global temperature evolution as illustrated in

535 Figure C1 Until year 2055, the forcing is the same as SSP5-8.5. From year 2056 – 2165, the temperature decreases similarly

536 to the increase between 2030 and 2055 but backwards at 0.25 the rate (drawing four years for one). From 2156 on we shuffle

537 and repeat the forcing earlier in the experiment, drawn from the time window 2026 – 2038.

538 Forcing until 2055 is the same as the corresponding SSP5-8.5 scenario. From 2056 – 2300 the following indices are used.

```
539  year = 2056, 2057, 2058, […], 2298, 2299, 2300 ;
540  shuffled_time_overshoot = 2056, 2056, 2055, 2054, 2053, 2055, 2054, 2053,
541     2052, 2054, 2053, 2052, 2051, 2053, 2052, 2051, 2050, 2052, 2051, 2050,
542     2049, 2051, 2050, 2049, 2048, 2050, 2049, 2048, 2047, 2049, 2048, 2047,
543     2046, 2048, 2047, 2046, 2045, 2047, 2046, 2045, 2044, 2046, 2045, 2044,
```

544   2043, 2045, 2044, 2043, 2042, 2044, 2043, 2042, 2041, 2043, 2042, 2041,
545   2040, 2042, 2041, 2040, 2039, 2041, 2040, 2039, 2038, 2040, 2039, 2038,
546   2037, 2039, 2038, 2037, 2036, 2038, 2037, 2036, 2035, 2037, 2036, 2035,
547   2034, 2036, 2035, 2034, 2033, 2035, 2034, 2033, 2032, 2034, 2033, 2032,
548   2031, 2033, 2032, 2031, 2030, 2032, 2031, 2030, 2029, 2033, 2038, 2031,
549   2037, 2029, 2035, 2028, 2034, 2036, 2030, 2027, 2032, 2035, 2031, 2037,
550   2029, 2030, 2033, 2032, 2034, 2028, 2038, 2027, 2036, 2032, 2031, 2027,
551   2037, 2034, 2033, 2036, 2035, 2029, 2030, 2038, 2028, 2027, 2034, 2029,
552   2030, 2033, 2036, 2031, 2032, 2035, 2038, 2028, 2037, 2034, 2038, 2027,
553   2036, 2037, 2029, 2035, 2031, 2030, 2032, 2033, 2028, 2036, 2031, 2027,
554   2032, 2030, 2038, 2028, 2034, 2035, 2033, 2029, 2037, 2036, 2028, 2030,
555   2027, 2038, 2032, 2037, 2033, 2034, 2029, 2031, 2035, 2028, 2030, 2035,
556   2033, 2029, 2037, 2034, 2031, 2038, 2032, 2027, 2036, 2032, 2031, 2027,
557   2030, 2028, 2034, 2037, 2035, 2033, 2036, 2038, 2029, 2029, 2036, 2035,
558   2033, 2037, 2028, 2027, 2031, 2038, 2034, 2032, 2030, 2038, 2027, 2033,
559   2037, 2030, 2034, 2036, 2028, 2031, 2029, 2032, 2035, 2038, 2027, 2030,
560   2031, 2034, 2035, 2037, 2036, 2032, 2029, 2033, 2028 ;
561
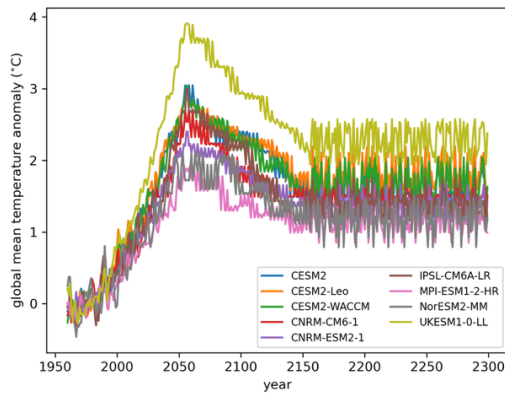
562
563   **Figure C1.** Illustration of the construction of schematic overshoot scenarios mimicking SSP5-3.4-OS. To construct the forcing, SMB and
564   retreat forcing are drawn from existing annual forcing files (not shown). Instead, the figure shows the sequence of global mean temperature
565   anomaly drawn from each individual original ESM temperature time series.

566   **Data Availability**

567   The forcing data will be provided in ISMIP6 format on a public archive. It consists of SMB and ST anomalies and their

568   respective vertical gradients that are generic for all ice sheet models. The retreat mask forcing is produced specifically for each

569   individual ice sheet model version and is maintained by the modellers.

570   For common analysis, ice sheet model output was conservatively interpolated to a standard 5 km diagnostic grid (same as

571   ISMIP6). These model output data will be made available on a public archive, while the raw ice sheet model output is the

572   responsibility of the individual modelling groups.

573   Projected sea-level contributions will be provided on a public archive.

574

Author contributions

HG designed the experimental setup with input from TE, prepared and distributed the forcing data, collected and processed the output data, analysed the results and produced the figures. XF, QG, MvdB, BN, RM, MO, FB produced climate forcing data. HG, CR, CJB, FGC and SL conducted ice sheet model experiments. HG wrote the manuscript with input from all co-authors.

Competing interests

At least one of the (co-)authors is a member of the editorial board of The Cryosphere.

Disclaimer

Publisher's note: Copernicus Publications remains neutral with regard to jurisdictional claims made in the text, published maps, institutional affiliations, or any other geographical representation in this paper. While Copernicus Publications makes every effort to include appropriate place names, the final responsibility lies with the authors.

Acknowledgements

We acknowledge the World Climate Research Programme and its Working Group on Coupled Modelling for coordinating and promoting CMIP5 and CMIP6. We thank the climate modelling groups for producing and making available their model output and the Earth System Grid Federation (ESGF) for archiving the CMIP data. We thank the ISMIP6/7 steering committee and community for defining and providing a framework for this work. Resources were provided by Sigma2 - the National Infrastructure for High Performance Computing and Data Storage in Norway through projects NN8085K, NN8006K, NS5011K, NS8006 K and NS8085K. B.N. is a Research Associate of the Fonds de la Recherche Scientifique de Belgique–F.R.S.-FNRS.

Financial support

This research has received funding from the European Union's Horizon 2020 research and innovation programme under grant agreement 869304 (PROTECT) and has been supported by the Research Council of Norway under project 324639 (GREASE).

References

Aschwanden, A., Bartholomaus, T. C., Brinkerhoff, D. J., and Truffer, M.: Brief communication: A roadmap towards credible projections of ice sheet contribution to sea level, The Cryosphere, 15, 5705–5715, https://doi.org/10.5194/tc-15-5705-2021, 2021.

Bales, R. C., Guo, Q., Shen, D., McConnell, J. R., Du, G., Burkhart, J. F., Spikes, V. B., Hanna, E., and Cappelen, J.: Annual accumulation for Greenland updated using ice core data developed during 2000–2006 and analysis of daily coastal meteorological data, Journal of Geophysical Research Atmospheres, 114, https://doi.org/10.1029/2008JD011208, 2009.

Berends, C. J., de Boer, B., and van de Wal, R. S. W.: Application of HadCM3@Bristolv1.0 simulations of paleoclimate as forcing for an ice-sheet model, ANICE2.1: set-up and benchmark experiments, Geosci. Model Dev., 11, 4657–4675, https://doi.org/10.5194/gmd-11-4657-2018, 2018.

Berends, C. J., Goelzer, H., Reerink, T. J., Stap, L. B., and van de Wal, R. S. W.: Benchmarking the vertically integrated ice-sheet model IMAU-ICE (version 2.0), Geosci. Model Dev., 15, 5667–5688, https://doi.org/10.5194/gmd-15-5667-2022, 2022.

Berends, C. J., Van De Wal, R. S. W., Van Den Akker, T., and Lipscomb, W. H.: Compensating errors in inversions for subglacial bed roughness: same steady state, different dynamic response, Cryosphere, 17, 1585–1600, https://doi.org/10.5194/tc-17-1585-2023, 2023.

Brady, E. C., Otto-Bliesner, B. L., Kay, J. E., and Rosenbloom, N.: Sensitivity to Glacial Forcing in the CCSM4, Journal of Climate, 26, 1901–1925, https://doi.org/10.1175/JCLI-D-11-00416.1, 2013.

Citterio, M. and Ahlstrøm, A. P.: Brief communication "The aerophotogrammetric map of Greenland ice masses," The Cryosphere, 7, 445–449, https://doi.org/10.5194/tc-7-445-2013, 2013.

Delhasse, A., Kittel, C., Amory, C., Hofer, S., van As, D., S. Fausto, R., and Fettweis, X.: Brief communication: Evaluation of the near-surface climate in ERA5 over the Greenland Ice Sheet, The Cryosphere, 14, 957–965, https://doi.org/10.5194/tc-14-957-2020, 2020.

Delhasse, A., Beckmann, J., Kittel, C., and Fettweis, X.: Coupling MAR (Modèle Atmosphérique Régional) with PISM (Parallel Ice Sheet Model) mitigates the positive melt–elevation feedback, The Cryosphere, 18, 633–651, https://doi.org/10.5194/tc-18-633-2024, 2024.

Durand, G., van den Broeke, M. R., Le Cozannet, G., Edwards, T. L., Holland, P. R., Jourdain, N. C., Marzeion, B., Mottram, R., Nicholls, R. J., Pattyn, F., Paul, F., Slangen, A. B. A., Winkelmann, R., Burgard, C., van Calcar, C. J., Barré, J.-B., Bataille, A., and Chapuis, A.: Sea-Level Rise: From Global Perspectives to Local Services, Frontiers in Marine Science, Volume 8-2021, 2022.

Edwards, T. L., Nowicki, S., Marzeion, B., Hock, R., Goelzer, H., Seroussi, H., Jourdain, N. C., Slater, D. A., Turner, F. E., Smith, C. J., McKenna, C. M., Simon, E., Abe-Ouchi, A., Gregory, J. M., Larour, E., Lipscomb, W. H., Payne, A. J., Shepherd, A., Agosta, C., Alexander, P., Albrecht, T., Anderson, B., Asay-Davis, X., Aschwanden, A., Barthel, A., Bliss, A., Calov, R., Chambers, C., Champollion, N., Choi, Y., Cullather, R., Cuzzone, J., Dumas, C., Felikson, D., Fettweis, X., Fujita, K., Galton-Fenzi, B. K., Gladstone, R., Golledge, N. R., Greve, R., Hattermann, T., Hoffman, M. J., Humbert, A., Huss, M., Huybrechts, P., Immerzeel, W., Kleiner, T., Kraaijenbrink, P., Le clec'h, S., Lee, V., Leguy, G. R., Little, C. M., Lowry, D. P., Malles, J. H., Martin, D. F., Maussion, F., Morlighem, M., O'Neill, J. F., Nias, I., Pattyn, F., Pelle, T., Price, S. F., Quiquet, A., Radić, V., Reese, R., Rounce, D. R., Rückamp, M., Sakai, A., Shafer, C., Schlegel, N. J., Shannon, S.,

Smith, R. S., Straneo, F., Sun, S., Tarasov, L., Trusel, L. D., Van Breedam, J., van de Wal, R., van den Broeke, M., Winkelmann, R., Zekollari, H., Zhao, C., Zhang, T., and Zwinger, T.: Projected land ice contributions to twenty-first-century sea level rise, Nature, 593, 74–82, https://doi.org/10.1038/s41586-021-03302-y, 2021.

Edwards, T. L. et al.: PROTECT sea-level projections. in prep, 2026.

Fettweis, X., Box, J. E., Agosta, C., Amory, C., Kittel, C., Lang, C., van As, D., Machguth, H., and Gallée, H.: Reconstructions of the 1900–2015 Greenland ice sheet surface mass balance using the regional climate MAR model, The Cryosphere, 11, 1015–1015, https://doi.org/10.5194/tc-11-1015-2017, 2017.

Fettweis, X., Hofer, S., Krebs-Kanzow, U., Amory, C., Aoki, T., Berends, C. J., Born, A., Box, J. E., Delhasse, A., Fujita, K., Gierz, P., Goelzer, H., Hanna, E., Hashimoto, A., Huybrechts, P., Kapsch, M.-L., King, M. D., Kittel, C., Lang, C., Langen, P. L., Lenaerts, J. T. M., Liston, G. E., Lohmann, G., Mernild, S. H., Mikolajewicz, U., Modali, K., Mottram, R. H., Niwano, M., Noël, B., Ryan, J. C., Smith, A., Streffing, J., Tedesco, M., van de Berg, W. J., van den Broeke, M., van de Wal, R. S. W., van Kampenhout, L., Wilton, D., Wouters, B., Ziemen, F., and Zolles, T.: GrSMBMIP: intercomparison of the modelled 1980–2012 surface mass balance over the Greenland Ice Sheet, The Cryosphere, 14, 3935–3958, https://doi.org/10.5194/tc-14-3935-2020, 2020.

Fox-Kemper, B., Hewitt, H. T., Xiao, C., Adalgeirsdottir, G., Drijfhout, S. S., Edwards, T. L., Golledge, N. R., Hemer, M., Kopp, R. E., Krinner, G., Mix, A., Notz, D., Nowicki, S., Nurhati, I. S., Ruiz, L., Sallee, J.-B., Slangen, A. B. A., and Yu, Y.: Climate Change 2021: The Physical Science Basis. Contribution of Working Group I to the Sixth Assessment Report of the Intergovernmental Panel on Climate Change, edited by: Masson-Delmotte, V., Zhai, P., Pirani, A., Connors, S. L., Péan, C., Berger, S., Caud, N., Chen, Y., Goldfarb, L., Gomis, M. I., Huang, M., Leitzell, K., Lonnoy, E., Matthews, J. B. R., Maycock, T. K., Waterfield, T., Yelekçi, O., Yu, R., and Zhou, B., Cambridge University Press, United Kingdom and New York, NY, USA, 1211–1362, https://doi.org/10.1017/9781009157896.011, 2021.

Franco, B., Fettweis, X., Lang, C., and Erpicum, M.: Impact of spatial resolution on the modelling of the Greenland ice sheet surface mass balance between 1990-2010, using the regional climate model MAR, Cryosphere, 6, 695–711, https://doi.org/10.5194/tc-6-695-2012, 2012.

Fürst, J. J., Goelzer, H., and Huybrechts, P.: Effect of higher-order stress gradients on the centennial mass evolution of the Greenland ice sheet, Cryosphere, 7, 183–199, https://doi.org/10.5194/tc-7-183-2013, 2013.

Fürst, J. J., Goelzer, H., and Huybrechts, P.: Ice-dynamic projections of the Greenland ice sheet in response to atmospheric and oceanic warming, Cryosphere, 9, 1039–1062, https://doi.org/10.5194/tc-9-1039-2015, 2015.

Gillet-Chaulet, F., Gagliardini, O., Seddik, H., Nodet, M., Durand, G., Ritz, C., Zwinger, T., Greve, R., and Vaughan, D. G.: Greenland ice sheet contribution to sea-level rise from a new-generation ice-sheet model, Cryosphere, 6, 1561–1576, https://doi.org/10.5194/tc-6-1561-2012, 2012.

Glaude, Q., Noel, B., Olesen, M., Van den Broeke, M., van de Berg, W. J., Mottram, R., Hansen, N., Delhasse, A., Amory, C., Kittel, C., Goelzer, H., and Fettweis, X.: A Factor Two Difference in 21st-Century Greenland Ice Sheet Surface Mass

Balance Projections From Three Regional Climate Models Under a Strong Warming Scenario (SSP5-8.5), Geophysical Research Letters, 51, e2024GL111902, https://doi.org/10.1029/2024GL111902, 2024.

Goelzer, H., Nowicki, S., Edwards, T., Beckley, M., Abe-Ouchi, A., Aschwanden, A., Calov, R., Gagliardini, O., Gillet-Chaulet, F., Golledge, N. R., Gregory, J., Greve, R., Humbert, A., Huybrechts, P., Kennedy, J. H., Larour, E., Lipscomb, W. H., Le clec'h, S., Lee, V., Morlighem, M., Pattyn, F., Payne, A. J., Rodehacke, C., Rückamp, M., Saito, F., Schlegel, N., Seroussi, H., Shepherd, A., Sun, S., van de Wal, R., and Ziemen, F. A.: Design and results of the ice sheet model initialisation experiments initMIP-Greenland: an ISMIP6 intercomparison, The Cryosphere, 12, 1433–1460, https://doi.org/10.5194/tc-12-1433-2018, 2018.

Goelzer, H., Nowicki, S., Payne, A., Larour, E., Seroussi, H., Lipscomb, W. H., Gregory, J., Abe-Ouchi, A., Shepherd, A., Simon, E., Agosta, C., Alexander, P., Aschwanden, A., Barthel, A., Calov, R., Chambers, C., Choi, Y., Cuzzone, J., Dumas, C., Edwards, T., Felikson, D., Fettweis, X., Golledge, N. R., Greve, R., Humbert, A., Huybrechts, P., Le clec'h, S., Lee, V., Leguy, G., Little, C., Lowry, D. P., Morlighem, M., Nias, I., Quiquet, A., Rückamp, M., Schlegel, N.-J., Slater, D. A., Smith, R. S., Straneo, F., Tarasov, L., van de Wal, R., and van den Broeke, M.: The future sea-level contribution of the Greenland ice sheet: a multi-model ensemble study of ISMIP6, The Cryosphere, 14, 3071–3096, https://doi.org/10.5194/tc-14-3071-2020, 2020a.

Goelzer, H., Coulon, V., Pattyn, F., de Boer, B., and van de Wal, R.: Brief communication: On calculating the sea-level contribution in marine ice-sheet models, The Cryosphere, 14, 833–840, https://doi.org/10.5194/tc-14-833-2020, 2020b.

Goelzer, H., Noël, B. P. Y., Edwards, T. L., Fettweis, X., Gregory, J. M., Lipscomb, W. H., van de Wal, R. S. W., and van den Broeke, M. R.: Remapping of Greenland ice sheet surface mass balance anomalies for large ensemble sea-level change projections, The Cryosphere, 14, 1747–1762, https://doi.org/10.5194/tc-14-1747-2020, 2020c.

Goelzer, H., Langebroek, P. M., Born, A., Hofer, S., Haubner, K., Petrini, M., Leguy, G., Lipscomb, W. H., and Thayer-Calder, K.: Interactive coupling of a Greenland ice sheet model in NorESM2, Geosci. Model Dev., 18, 7853–7867, https://doi.org/10.5194/gmd-18-7853-2025, 2025.

Goldberg, D. N.: A variationally derived, depth-integrated approximation to a higher-order glaciological flow model, Journal of Glaciology, 57, 157–170, https://doi.org/10.3189/002214311795306763, 2011.

Hersbach, H., Bell, B., Berrisford, P., Hirahara, S., Horányi, A., Muñoz-Sabater, J., Nicolas, J., Peubey, C., Radu, R., Schepers, D., Simmons, A., Soci, C., Abdalla, S., Abellan, X., Balsamo, G., Bechtold, P., Biavati, G., Bidlot, J., Bonavita, M., De Chiara, G., Dahlgren, P., Dee, D., Diamantakis, M., Dragani, R., Flemming, J., Forbes, R., Fuentes, M., Geer, A., Haimberger, L., Healy, S., Hogan, R. J., Hólm, E., Janisková, M., Keeley, S., Laloyaux, P., Lopez, P., Lupu, C., Radnoti, G., de Rosnay, P., Rozum, I., Vamborg, F., Villaume, S., and Thépaut, J.-N.: The ERA5 global reanalysis, Quarterly Journal of the Royal Meteorological Society, 146, 1999–2049, https://doi.org/10.1002/qj.3803, 2020.

Hofer, S., Lang, C., Amory, C., Tedstone, A., Fettweis, X., Kittel, C., and Delhasse, A.: Greater Greenland Ice Sheet contribution to global sea level rise in CMIP6, Nature Communications, 1–11, https://doi.org/10.1038/s41467-020-20011-8, 2020.

Howat, I. M., Negrete, A., and Smith, B. E.: The Greenland Ice Mapping Project (GIMP) land classification and surface elevation data sets, The Cryosphere, 8, 1509–1518, https://doi.org/10.5194/tc-8-1509-2014, 2014.

Huybrechts, P.: Sea-level changes at the LGM from ice-dynamic reconstructions of the Greenland and Antarctic ice sheets during the glacial cycles, Quaternary Science Reviews, 21, 203–231, https://doi.org/10.1016/S0277-3791(01)00082-8, 2002.

Huybrechts, P., Gregory, J. M., Janssens, I., and Wild, M.: Modelling Antarctic and Greenland volume changes during the 20th and 21st centuries forced by GCM time slice integrations, Global and Planetary Change, 42, 83–105, https://doi.org/10.1016/j.gloplacha.2003.11.011, 2004.

Joughin, I., Smith, B. E., Howat, I. M., Scambos, T., and Moon, T.: Greenland flow variability from ice-sheet-wide velocity mapping, Journal of Glaciology, 56, 415–430, https://doi.org/10.3189/002214310792447734, 2010.

Langen, P. L., Fausto, R. S., Vandecrux, B., Mottram, R. H., and Box, J. E.: Liquid Water Flow and Retention on the Greenland Ice Sheet in the Regional Climate Model HIRHAM5: Local and Large-Scale Impacts, Frontiers in Earth Science, Volume 4-2016, 2017.

Le clec'h, S., Quiquet, A., Charbit, S., Dumas, C., Kageyama, M., and Ritz, C.: A rapidly converging initialisation method to simulate the present-day Greenland ice sheet using the GRISLI ice sheet model (version 1.3), Geosci. Model Dev., 12, 2481–2499, https://doi.org/10.5194/gmd-12-2481-2019, 2019.

Lipscomb, W. H., Price, S. F., Hoffman, M. J., Leguy, G. R., Bennett, A. R., Bradley, S. L., Evans, K. J., Fyke, J. G., Kennedy, J. H., Perego, M., Ranken, D. M., Sacks, W. J., Salinger, A. G., Vargo, L. J., and Worley, P. H.: Description and evaluation of the Community Ice Sheet Model (CISM) v2.1, Geoscientific Model Development, 12, 387–424, https://doi.org/10.5194/gmd-12-387-2019, 2019.

MacFarling Meure, C., Etheridge, D., Trudinger, C., Steele, P., Langenfelds, R., van Ommen, T., Smith, A., and Elkins, J.: Law Dome CO2, CH4 and N2O ice core records extended to 2000 years BP, Geophysical Research Letters, 33, https://doi.org/10.1029/2006GL026152, 2006.

Morlighem, M., Williams, C. N., Rignot, E., An, L., Arndt, J. E., Bamber, J. L., Catania, G., Chauché, N., Dowdeswell, J. A., Dorschel, B., Fenty, I., Hogan, K., Howat, I., Hubbard, A., Jakobsson, M., Jordan, T. M., Kjeldsen, K. K., Millan, R., Mayer, L., Mouginot, J., Noël, B. P. Y. Y., O'Cofaigh, C., Palmer, S., Rysgaard, S., Seroussi, H., Siegert, M. J., Slabon, P., Straneo, F., van den Broeke, M. R., Weinrebe, W., Wood, M., Zinglersen, K. B., Cofaigh, C. Ó., Palmer, S., Rysgaard, S., Seroussi, H., Siegert, M. J., Slabon, P., Straneo, F., van den Broeke, M. R., Weinrebe, W., Wood, M., and Zinglersen, K. B.: BedMachine v3: Complete bed topography and ocean bathymetry mapping of Greenland from multi-beam echo sounding combined with mass conservation, Geophysical Research Letters, 44, 11,051-11,061, https://doi.org/10.1002/2017GL074954, 2017.

Mottram, R., Boberg, F., Langen, P., Yang, S., Rodehacke, C., Christensen, J. H., and Madsen, M. S.: Surface mass balance of the Greenland ice sheet in the regional climate model HIRHAM5: Present state and future prospects, Low Temperature Science, 75, 105–115, https://doi.org/10.14943/lowtemsci.75.105, 2017.

Muntjewerf, L., Petrini, M., Vizcaino, M., Ernani da Silva, C., Sellevold, R., Scherrenberg, M. D. W., Thayer-Calder, K., Bradley, S. L., Lenaerts, J. T. M., Lipscomb, W. H., and Lofverstrom, M.: Greenland Ice Sheet Contribution to 21st Century Sea Level Rise as Simulated by the Coupled CESM2.1-CISM2.1, Geophysical Research Letters, 47, https://doi.org/10.1029/2019GL086836, 2020.

Noël, B., van de Berg, W. J., Machguth, H., Lhermitte, S., Howat, I., Fettweis, X., and van den Broeke, M. R.: A daily, 1 km resolution data set of downscaled Greenland ice sheet surface mass balance (1958–2015), The Cryosphere, 10, 2361–2377, https://doi.org/10.5194/tc-10-2361-2016, 2016.

Noël, B., Van De Berg, W. J., Van Wessem, J. M., Van Meijgaard, E., Van As, Di., Lenaerts, J. T. M., Lhermitte, S., Munneke, P. K., Smeets, C. J. P. P., Van Ulft, L. H., Van De Wal, R. S. W., and Van Den Broeke, M. R.: Modelling the climate and surface mass balance of polar ice sheets using RACMO2 - Part 1: Greenland (1958-2016), Cryosphere, 12, 811–831, https://doi.org/10.5194/tc-12-811-2018, 2018.

Noël, B., van Kampenhout, L., van de Berg, W. J., Lenaerts, J. T. M., Wouters, B., and van den Broeke, M. R.: Brief communication: CESM2 climate forcing (1950–2014) yields realistic Greenland ice sheet surface mass balance, The Cryosphere, 14, 1425–1435, https://doi.org/10.5194/tc-14-1425-2020, 2020.

Noël, B., Lenaerts, J. T. M., Lipscomb, W. H., Thayer-Calder, K., and van den Broeke, M. R.: Peak refreezing in the Greenland firn layer under future warming scenarios, Nature Communications, 13, 6870, https://doi.org/10.1038/s41467-022-34524-x, 2022.

Nowicki, S. M. J., Payne, A., Larour, E., Seroussi, H., Goelzer, H., Lipscomb, W., Gregory, J., Abe-Ouchi, A., and Shepherd, A.: Ice Sheet Model Intercomparison Project (ISMIP6) contribution to CMIP6, Geoscientific Model Development, 9, 4521–4545, https://doi.org/10.5194/gmd-9-4521-2016, 2016.

Nowicki, S., Payne, A. J., Goelzer, H., Seroussi, H., Lipscomb, W. H., Abe-Ouchi, A., Agosta, C., Alexander, P., Asay-Davis, X. S., Barthel, A., Bracegirdle, T. J., Cullather, R., Felikson, D., Fettweis, X., Gregory, J., Hatterman, T., Jourdain, N. C., Kuipers Munneke, P., Larour, E., Little, C. M., Morlighem, M., Nias, I., Shepherd, A., Simon, E., Slater, D., Smith, R., Straneo, F., Trusel, L. D., van den Broeke, M. R., and van de Wal, R.: Experimental protocol for sealevel projections from ISMIP6 standalone ice sheet models, The Cryosphere, 14, 2331-2368-2331–2368, https://doi.org/10.5194/tc-14-2331-2020, 2020.

O'Neill, B. C., Tebaldi, C., van Vuuren, D. P., Eyring, V., Friedlingstein, P., Hurtt, G., Knutti, R., Kriegler, E., Lamarque, J.-F., Lowe, J., Meehl, G. A., Moss, R., Riahi, K., and Sanderson, B. M.: The Scenario Model Intercomparison Project (ScenarioMIP) for CMIP6, Geosci. Model Dev., 9, 3461–3482, https://doi.org/10.5194/gmd-9-3461-2016, 2016.

Payne, A. J., Nowicki, S., Abe-Ouchi, A., Agosta, C., Alexander, P., Albrecht, T., Asay-Davis, X., Aschwanden, A., Barthel, A., Bracegirdle, T. J., Calov, R., Chambers, C., Choi, Y., Cullather, R., Cuzzone, J., Dumas, C., Edwards, T. L., Felikson, D., Fettweis, X., Galton-Fenzi, B. K., Goelzer, H., Gladstone, R., Golledge, N. R., Gregory, J. M., Greve, R., Hattermann, T., Hoffman, M. J., Humbert, A., Huybrechts, P., Jourdain, N. C., Kleiner, T., Munneke, P. K., Larour, E., Le clec'h, S., Lee, V., Leguy, G., Lipscomb, W. H., Little, C. M., Lowry, D. P., Morlighem, M., Nias, I., Pattyn, F., Pelle, T., Price, S.

F., Quiquet, A., Reese, R., Rückamp, M., Schlegel, N. J., Seroussi, H., Shepherd, A., Simon, E., Slater, D., Smith, R. S., Straneo, F., Sun, S., Tarasov, L., Trusel, L. D., Van Breedam, J., van de Wal, R., van den Broeke, M., Winkelmann, R., Zhao, C., Zhang, T., and Zwinger, T.: Future Sea Level Change Under Coupled Model Intercomparison Project Phase 5 and Phase 6 Scenarios From the Greenland and Antarctic Ice Sheets, Geophysical Research Letters, 48, 1–8, https://doi.org/10.1029/2020GL091741, 2021.

Rahlves, C., Goelzer, H., Born, A., and Langebroek, P. M.: Historically consistent mass loss projections of the Greenland ice sheet, The Cryosphere, 19, 1205–1220, https://doi.org/10.5194/tc-19-1205-2025, 2025a.

Rahlves, C., Goelzer, H., Born, A., and Langebroek, P. M.: Investigating the multi-millennial evolution and stability of the Greenland ice sheet using remapped surface mass balance forcing, EGUsphere, 2025, 1–23, https://doi.org/10.5194/egusphere-2025-2192, 2025b.

Rantanen, M., Karpechko, A. Yu., Lipponen, A., Nordling, K., Hyvärinen, O., Ruosteenoja, K., Vihma, T., and Laaksonen, A.: The Arctic has warmed nearly four times faster than the globe since 1979, Communications Earth & Environment, 3, 168, https://doi.org/10.1038/s43247-022-00498-3, 2022.

Rohmer, J., Thieblemont, R., Le Cozannet, G., Goelzer, H., and Durand, G.: Improving interpretation of sea-level projections through a machine-learning-based local explanation approach, The Cryosphere, 16, 4637–4657, https://doi.org/10.5194/tc-16-4637-2022, 2022.

Rohmer, J., Goelzer, H., Edwards, T., Le Cozannet, G., and Durand, G.: Drawing lessons for multi-model ensemble design from emulator experiments: application to future sea level contribution of the Greenland ice sheet, EGUsphere [preprint], https://doi.org/10.5194/egusphere-2025-52, 2025.

Scherrenberg, M. D. W., Berends, C. J., Stap, L. B., and Van De Wal, R. S. W.: Modelling feedbacks between the Northern Hemisphere ice sheets and climate during the last glacial cycle, Climate of the Past, 19, 399–418, https://doi.org/10.5194/cp-19-399-2023, 2023.

Schoof, C.: The effect of cavitation on glacier sliding, Proceedings of the Royal Society A: Mathematical, Physical and Engineering Sciences, 461, 609–627, https://doi.org/10.1098/rspa.2004.1350, 2005.

Shapiro, N. M. and Ritzwoller, M. H.: Inferring surface heat flux distributions guided by a global seismic model: particular application to Antarctica, Earth and Planetary Science Letters, 223, 213–224, https://doi.org/10.1016/j.epsl.2004.04.011, 2004.

Singarayer, J. S. and Valdes, P. J.: High-latitude climate sensitivity to ice-sheet forcing over the last 120kyr, Quaternary Science Reviews, 29, 43–55, https://doi.org/10.1016/j.quascirev.2009.10.011, 2010.

Slater, D. A., Straneo, F., Felikson, D., Little, C. M., Goelzer, H., Fettweis, X., and Holte, J.: Estimating Greenland tidewater glacier retreat driven by submarine melting, The Cryosphere, 13, 2489–2509, https://doi.org/10.5194/tc-13-2489-2019, 2019.

Slater, D. A., Felikson, D., Straneo, F., Goelzer, H., Little, C. M., Morlighem, M., Fettweis, X., and Nowicki, S.: Twenty-first century ocean forcing of the Greenland ice sheet for modelling of sea level contribution, The Cryosphere, 14, 985–1008, https://doi.org/10.5194/tc-14-985-2020, 2020.

Smith, R. S., Mathiot, P., Siahaan, A., Lee, V., Cornford, S. L., Gregory, J. M., Payne, A. J., Jenkins, A., Holland, P. R., Ridley, J. K., and Jones, C. G.: Coupling the U.K. Earth System Model to Dynamic Models of the Greenland and Antarctic Ice Sheets, Journal of Advances in Modeling Earth Systems, 13, e2021MS002520, https://doi.org/10.1029/2021MS002520, 2021.

The IMBIE Team, Shepherd, A., Ivins, E., Rignot, E., Smith, B., van den Broeke, M., Velicogna, I., Whitehouse, P., Briggs, K., Joughin, I., Krinner, G., Nowicki, S., Payne, T., Scambos, T., Schlegel, N., A, G., Agosta, C., Ahlstrøm, A., Babonis, G., Barletta, V. R., Bjørk, A. A., Blazquez, A., Bonin, J., Colgan, W., Csatho, B., Cullather, R., Engdahl, M. E., Felikson, D., Fettweis, X., Forsberg, R., Hogg, A. E., Gallee, H., Gardner, A., Gilbert, L., Gourmelen, N., Groh, A., Gunter, B., Hanna, E., Harig, C., Helm, V., Horvath, A., Horwath, M., Khan, S., Kjeldsen, K. K., Konrad, H., Langen, P. L., Lecavalier, B., Loomis, B., Luthcke, S., McMillan, M., Melini, D., Mernild, S., Mohajerani, Y., Moore, P., Mottram, R., Mouginot, J., Moyano, G., Muir, A., Nagler, T., Nield, G., Nilsson, J., Noël, B., Otosaka, I., Pattle, M. E., Peltier, W. R., Pie, N., Rietbroek, R., Rott, H., Sandberg Sørensen, L., Sasgen, I., Save, H., Scheuchl, B., Schrama, E., Schröder, L., Seo, K. W., Simonsen, S. B., Slater, T., Spada, G., Sutterley, T., Talpe, M., Tarasov, L., van de Berg, W. J., van der Wal, W., van Wessem, M., Vishwakarma, B. D., Wiese, D., Wilton, D., Wagner, T., Wouters, B., and Wuite, J.: Mass balance of the Greenland Ice Sheet from 1992 to 2018, Nature, 579, 233–239, https://doi.org/10.1038/s41586-019-1855-2, 2020.

van den Broeke, M., Box, J., Fettweis, X., Hanna, E., Noël, B., Tedesco, M., van As, D., van de Berg, W. J., and van Kampenhout, L.: Greenland Ice Sheet Surface Mass Loss: Recent Developments in Observation and Modeling, Current Climate Change Reports, 3, 345–356, https://doi.org/10.1007/s40641-017-0084-8, 2017.